Rescattering and chiral dynamics in $B \to \rho\pi$ decay

S. Gardner*
Department of Physics and Astronomy, University of Kentucky, Lexington, Kentucky 40506-0055

Ulf-G. Meißner†
Forschungszentrum Jülich, Institut für Kernphysik (Theorie), D-52425 Jülich, Germany

(Received 24 December 2001; published 15 April 2002)

We examine the role of $B^0(\overline{B}^0) \to \sigma\pi^0 \to \pi^+\pi^-\pi^0$ decay in the Dalitz plot analysis of $B^0(\overline{B}^0) \to \rho\pi \to \pi^+\pi^-\pi^0$ decays, employed to extract the CKM parameter α. The $\sigma\pi$ channel is significant because it can break the relationship between the penguin contributions in $B \to \rho^0\pi^0$, $B \to \rho^+\pi^-$, and $B \to \rho^-\pi^+$ decays consequent to an assumption of isospin symmetry. Its presence thus mimics the effect of isospin violation. The $\sigma\pi^0$ state is of definite CP, however; we demonstrate that the $B \to \rho\pi$ analysis can be generalized to include this channel without difficulty. The σ or $f_0(400-1200)$ ''meson'' is a broad $I=J=0$ enhancement driven by strong $\pi\pi$ rescattering; a suitable scalar form factor is constrained by the chiral dynamics of low-energy hadron-hadron interactions—it is rather different from the relativistic Breit-Wigner form adopted in earlier $B \to \sigma\pi$ and $D \to \sigma\pi$ analyses. We show that the use of this scalar form factor leads to an improved theoretical understanding of the measured ratio $\mathrm{Br}(\overline{B}^0 \to \rho^{\mp}\pi^{\pm})/\mathrm{Br}(B^- \to \rho^0\pi^-)$.

DOI: 10.1103/PhysRevD.65.094004 PACS number(s): 13.25.Hw, 11.30.Er, 12.39.Fe, 14.40.Cs

I. INTRODUCTION

Measurements at SLAC and KEK of the time-dependent CP-violating asymmetry in $B(\overline{B}) \to J/\psi K_s$ [1,2], yielding $\sin(2\beta)$, have conclusively established the existence of CP violation in the B meson system. The results found are consistent with standard model (SM) expectations [3], so that establishing whether or not the Cabibbo-Kobayashi-Maskawa (CKM) matrix [4] is the only source of CP violation in nature, as in the SM, requires the empirical measurement of all the angles of the unitarity triangle.

In this paper we consider the determination of α through a Dalitz plot analysis of the decays $B^0(\overline{B}^0) \to \rho\pi \to \pi^+\pi^-\pi^0$ under the assumption of isospin symmetry [5,6]. Ten parameters appear in the analysis, and they can be determined in a fit to the data. Nevertheless, the assumption of ρ dominance in $B \to 3\pi$ decays has no strong theoretical basis [7], so that the contributions from other resonances in the $\rho\pi$ phase space may be important. We discuss how the isospin analysis can be enlarged to include the $\sigma\pi$ channel as well. The σ or $f_0(400-1200)$ ''meson'' is a broad $J=I=0$ enhancement, close to the ρ meson in mass, so that the $\sigma\pi$ channel can potentially populate the 3π phase space associated with the $\rho\pi$ channels. The $\sigma\pi$ final state contributes preferentially to the $\rho^0\pi^0$ final state. In the context of the isospin analysis, such contributions are of consequence as they invalidate the underlying assumptions of the isospin analysis and thus mimic the effect of isospin violation.

Our considerations are inspired in part by recent studies of $D^- \to \pi^-\pi^+\pi^-$ decay: the E791 Collaboration find that the pathway $D^- \to \pi^-\sigma \to \pi^-\pi^+\pi^-$ accounts for approximately half of all $D^- \to \pi^-\pi^+\pi^-$ decays [8]. Deandrea and Polosa have argued as a consequence that the $B \to \sigma\pi$ channel contributes significantly to the $\rho\pi$ phase space in $B \to \pi\pi^+\pi^-$ and modifies the ratio $\mathcal{B}(\overline{B}^0 \to \rho^{\mp}\pi^{\pm})/\mathcal{B}(B^- \to \rho^0\pi^-)$ to yield better agreement with experiment [9]. The scalar form factor, which describes the appearance of the σ in the $\pi^+\pi^-$ final state, enters as a crucial ingredient in the assessment of the size of these effects. The scalar form factor cannot be determined directly from experiment; nevertheless, ample indirect constraints exist, permitting us to describe its features with confidence [10]. Nevertheless, different approaches, with different dynamical assumptions, yield roughly comparable descriptions of the $\pi\pi$ scattering data, so that the emergence of a favored form of the scalar form factor does not resolve the question of whether the σ is a pre-existing resonance or, rather, a dynamical consequence of $\pi\pi$ interactions in the final state. We follow Ref. [10] and adopt a unitarized, coupled-channel approach to the final-state interactions (FSI) in the $\pi\pi$-$K\overline{K}$ system, and match the resulting scalar form factor to chiral perturbation theory (CHPT) in the regime where the latter is applicable. The resulting form factor, in the $\pi\pi$ channel, discussed in Sec. V, is strikingly different from the relativistic Breit-Wigner form adopted by the E791 Collaboration in their analysis of the σ in $D^+ \to \pi^+\pi^+\pi^-$ decay—the latter form factor is also used in Ref. [9]. The differences are particularly large as $\sqrt{s} \to 2M_\pi$, so that the relativistic Breit-Wigner form is at odds with CHPT in the precise region where it is applicable, note Fig. 4 in Ref. [10]. This casts doubt on the recent conclusions of Refs. [8,9], prompting new analyses incorporating a suitable scalar form factor.

The generation of the σ resonance via strong rescattering effects, as in the approach we adopt, indicates that Okubo-Zweig-Iizuka- (OZI-)violating effects in the scalar sector are significant. Moreover, the ''doubly'' OZI-violating form factor $\langle 0|\overline{ss}|\pi\pi\rangle$ is non-trivial as well; such a contribution is

*Electronic address: gardner@pa.uky.edu
†Electronic address: u.meissner@fz-juelich.de

needed to fit the $\pi\pi$ and $K\bar{K}$ invariant mass distributions in $J/\psi \to \phi\pi\pi(K\bar{K})$ decay [10]. These effects are also needed to explain the branching ratios of the decays of the $a_0(980)$ and $f_0(980)$ states into $\pi\pi$ and KK final states [11]. These observations give new insight on rescattering effects in hadronic B decays, generating a new mechanism of factorization breaking in $n \geqslant 3$ particle final states.

The contribution of the $B \to \sigma\pi$ channel to the $B \to \rho^0\pi$ phase space can also modify the inferred empirical branching ratios in these channels. Combining the CLEO results [12]

$$\mathrm{Br}(B^- \to \rho^0\pi^-) = (10.4^{+3.3}_{-3.4} \pm 2.1) \times 10^{-6}, \tag{1}$$

$$\mathrm{Br}(\bar{B}^0 \to \rho^\pm\pi^\mp) = (27.6^{+8.4}_{-7.4} \pm 4.2) \times 10^{-6} \tag{2}$$

with the BaBar result [13] $\mathrm{Br}(B^0 \to \rho^\pm\pi^\mp) = 28.9 \pm 5.4 \pm 4.3$ (charge conjugate modes are implied) yields, adding the errors in quadrature and ignoring correlations,

$$\mathcal{R} = \frac{\mathrm{Br}(\bar{B}^0 \to \rho^\mp\pi^\pm)}{\mathrm{Br}(B^- \to \rho^0\pi^-)} = 2.7 \pm 1.2. \tag{3}$$

This ratio of ratios is roughly 6 if one works at tree level and uses the naive factorization approximation for the hadronic matrix elements [14]. The inclusion of penguin contributions can alter this result, and potentially yield better accord with theory and experiment [15–18]. However, our focus will parallel that of Ref. [9]: we wish to examine how $B \to \sigma\pi \to 3\pi$ decay, given a particular scalar form factor, can effectively modify the theoretical prediction of the ratio given in Eq. (3). It is apparent that $B \to \sigma\pi$ is of greater impact in $B \to \rho^0\pi$ decay, so that the inclusion of such contributions ought alter the ratio of ratios.

We begin by reviewing the isospin analysis in $B^0(\bar{B}^0) \to \rho\pi \to \pi^+\pi^-\pi^0$ decay [5,6] in Sec. II, and discuss its extension to include $B^0(\bar{B}^0) \to \sigma\pi \to \pi^+\pi^-\pi^0$) decay in Sec. III. We proceed by evaluating σ-mediated $B \to 3\pi$ decay in Sec. IV, relegating the ρ-mediated $B \to 3\pi$ decay formulas to the Appendix. Our analysis employs the scalar and vector form factors discussed in Sec. V and Sec. VI, respectively. We conclude with a presentation of our results in Sec. VII and an accompanying summary.

II. PRELIMINARIES: ISOSPIN ANALYSIS OF $B \to \rho\pi$

Let us recall the isospin analysis possible in $B \to \rho\pi$ decay [5,6]. Under the assumption of isospin symmetry, a $\rho\pi$ final state can have isospin $I_f = 0,1$, or 2, whereas the B^+, B^0 states form an isospin doublet. Thus we can have $|\Delta I| = 1/2,3/2$, or 5/2 transitions in $B \to \rho\pi$ decay, so that we can parametrize the amplitudes which appear by $A_{|\Delta I|, I_f}$. We have [5,19][1]

$$a_{+-} \equiv A(B^0 \to \rho^+\pi^-) = \frac{1}{2\sqrt{3}}[A_{3/2,2} + A_{5/2,2}] + \frac{1}{2}[A_{3/2,1} + A_{1/2,1}] + \frac{1}{\sqrt{6}}A_{1/2,0}, \tag{4}$$

$$a_{-+} \equiv A(B^0 \to \rho^-\pi^+) = \frac{1}{2\sqrt{3}}[A_{3/2,2} + A_{5/2,2}] - \frac{1}{2}[A_{3/2,1} + A_{1/2,1}] + \frac{1}{\sqrt{6}}A_{1/2,0}, \tag{5}$$

and

$$a_{00} \equiv A(B^0 \to \rho^0\pi^0) = -\frac{1}{\sqrt{3}}[A_{3/2,2} + A_{5/2,2}] + \frac{1}{\sqrt{6}}A_{1/2,0}, \tag{6}$$

noting that $A(B^0 \to \pi^+\pi^-\pi^0) = f_+ a_{+-} + f_- a_{-+} + f_0 a_{00}$, where f_i is the form factor describing $\rho^i \to \pi\pi$. Isospin is merely an approximate symmetry of the SM; nevertheless, our parametrization possesses three independent ''isospin'' amplitudes, distinguished by I_f, to describe the three empirical amplitudes a_{ij}, so that it persists in the presence of isospin breaking as well.

The lowest-dimension operators of the effective, $|\Delta B| = 1$ Hamiltonian generate transitions of $|\Delta I| = 1/2$ or 3/2 character, so that a $|\Delta I| = 5/2$ transition is generated, in this order, through long-distance, isospin-breaking effects in concert with a $|\Delta I| = 1/2$ or 3/2, short-distance, weak transition. If we neglect transitions of $|\Delta I| = 5/2$ character and, indeed, isospin-violating effects all together, the transition $\bar{b} \to q\bar{q}d$ which mediates $B \to \rho\pi$ decay can be realized through a ''tree'' amplitude with $|\Delta I| = 1/2$ or 3/2 or through a ''penguin'' amplitude with $|\Delta I| = 1/2$. Practically, the decay topologies are distinguished by their weak phase, so that the contributions associated with the CKM factors $V^*_{ub}V_{ud}$, e.g., are defined to be tree contributions, regardless of their dynamical origin. The unitarity of the CKM matrix in the SM implies that two combinations of CKM factors suffice in describing $b \to q\bar{q}q'$; here we associate the combination $V^*_{tb}V_{td}$ with the penguin contribution. Noting

$$\frac{V^*_{ub}V_{ud}}{|V^*_{ub}V_{ud}|} = e^{i\gamma}, \qquad \frac{V^*_{tb}V_{td}}{|V^*_{tb}V_{td}|} = e^{-i\beta} \tag{7}$$

and $\alpha = \pi - \beta - \gamma$, we have

$$e^{i\beta}a_{+-} = T^{+-}e^{-i\alpha} + P^{+-}, \quad e^{i\beta}a_{-+} = T^{-+}e^{-i\alpha} + P^{-+}, \quad e^{i\beta}a_{00} = T^{00}e^{-i\alpha} + P^{00}. \tag{8}$$

The overall weak phase $e^{i\beta}$ is without physical impact and can be neglected, because in the SM the weak phase associ-

[1] We flip the overall sign of the a_{00} amplitude with respect to Ref. [19], to conform with our computation of the amplitudes.

ated with $B^0-\overline{B}^0$ mixing is controlled by $q/p=\exp(-2i\beta)$.[2] Thus $q\overline{a}_{ij}/p\propto\exp(-i\beta)$, just as a_{ij} is. Consequently, the isospin analysis in $B\to\rho\pi$ decay determines α. The crucial assumption of the isospin analysis is to associate the CKM factor $V_{tb}^*V_{td}$ with $|\Delta I|=1/2$ transitions exclusively, so that from Eqs. (4), (5), (6), we have

$$P^{00}=\frac{1}{2}(P^{+-}+P^{-+}). \tag{9}$$

The overall strong phase in Eq. (8) is trivial, so that with Eq. (9), we have ten parameters in all, which can be determined in an analysis of the Dalitz plot [6,19].

The presence of the $\sigma\pi$ final state in the phase space associated with the $\rho^0\pi^0$ channel breaks the relation assumed in Eq. (9), and thus mimics the appearance of isospin violation. In this paper we study how the impact of this additional decay channel can be minimized. It is worth noting, however, that the $\sigma\pi$ final state is of definite CP, so that the isospin analysis can be enlarged to include this channel as well—additional observables are also present in this case. Before doing this, let us enumerate the ways in which SM isospin violation can impact the usual $B\to\rho\pi$ analysis, to determine whether the impact of these effects can be reduced as well:

(i) Isospin violation can generate an additional amplitude, of $|\Delta I|=5/2$ character, as in Eqs. (4), (5), (6). A $|\Delta I|=5/2$ amplitude can be generated by $\mathcal{O}(m_d-m_u)$ or $\mathcal{O}(\alpha)$ effects in concert with a $|\Delta I|=3/2$ weak transition, or by $\mathcal{O}(\alpha)$ effects in concert with a $|\Delta I|=1/2$ weak transition. The $\mathcal{O}(m_d-m_u)$ term acts as an isovector interaction. We recall that the physical neutral pion state is an admixture of the pseudoscalar octet fields π^0 and η; that is, $(\pi^0)_{\rm phys}=\pi^0+\epsilon\eta$ with $\epsilon\sim\mathcal{O}(m_d-m_u)$. Consequently ϵ acts as an $I=1$ ''spurion'' [20], encoding isospin-violating effects so that the matrix elements with the spurion are $SU(2)_f$ invariant. Isospin violation is also realized via the B^+, B^0 mass difference; such effects are not encoded in the spurion framework, but they are also comparatively trivial.

(ii) Isospin violation can modify the form factors f_i. The factor f_0, e.g., is distinguished by the G-parity-violating decay $\omega\to\pi^+\pi^-$. The magnitude and phase of this effective ρ^0-ω ''mixing'' can be elucidated from $e^+e^-\to\pi^+\pi^-$ data [21]; however, the contribution is reflective of the decay $B^0\to\omega\pi^0\to\pi^+\pi^-\pi^0$, so that a_{00} is modified in this region as well. In addition, electromagnetic effects distinguish $f_{\mp}$, probed in τ decay, from f_0 [22,23].

(iii) Penguin contributions of $|\Delta I|=3/2$ character can occur, either through electroweak penguin effects [24], or through isospin violation in the matrix elements of the gluonic penguin operator [25–27].

[2]Recall that the B mass eigenstates are defined via $|B_L\rangle=p|B^0\rangle+q|\overline{B}^0\rangle$ and $|B_H\rangle=p|B^0\rangle-q|\overline{B}^0\rangle$. We assume throughout that the width difference of the two B mass eigenstates is negligible, so that $|q/p|=1$.

The impact of these isospin-violating effects can be redressed, at least in part. For example, in $B\to\rho\pi$ decay, the $A_{5/2,2}$ amplitude appears in the combination $A_{5/2,2}+A_{3/2,2}$ throughout Eqs. (4), (5), (6). Moreover, the two amplitudes share the same weak phase, to a good approximation. This emerges because, unlike $K\to\pi\pi$ decay [28], no ''$|\Delta I|=1/2$ rule'' apparently exists in $B\to\pi\pi$ decay—though $\mathcal{B}(B^+\to\pi^+\pi^0)$ has yet to be conclusively determined [29]. Recent theoretical estimates suggest that the magnitude of the ratio of the $|\Delta I|=1/2$ to $|\Delta I|=3/2$ amplitudes in $B\to\pi\pi$ decay is roughly 0.3 [30], so that the $|\Delta I|=5/2$ amplitude is driven by an underlying $|\Delta I|=3/2$ weak transition. Strong-interaction isospin violation acts in concert with a $|\Delta I|=3/2$ weak transition to generate a $|\Delta I|=5/2$ amplitude, whereas electromagnetism can generate a $|\Delta I|=5/2$ amplitude from a $|\Delta I|=1/2$ weak transition. The size of strong-interaction isospin violation is typified by the $\pi^0-\eta$ mixing angle $\epsilon^{(2)}=\sqrt{3}(m_d-m_u)/4(m_s-\hat{m})$ with $\hat{m}=(m_d+m_u)/2$; we note that $\epsilon^{(2)}/\alpha\sim1.45$ [31], enhancing the extent to which $A_{5/2,2}$ and $A_{3/2,2}$ share the same weak phase. To the degree that this is true, the phenomenological T^{ij} parameters of Eq. (8) include $|\Delta I|=5/2$ effects as well. Thus we see that the single, crucial assumption of the isospin analysis is that the CKM factor $V_{tb}^*V_{td}$ accompanies $|\Delta I|=1/2$ transitions exclusively, for in this case the weak phases of the $A_{5/2,2}$ and $A_{3/2,2}$ amplitudes are identical. We have shown that isospin-violating contributions built on the $|\Delta I|=3/2$ short-distance, weak transition do not impact the isospin analysis in $B\to\rho\pi$. However, non-$|\Delta I|=1/2$ penguin effects, be they electroweak penguin contributions or contributions consequent to isospin-violating effects in the hadronic matrix elements of $|\Delta I|=1/2$ operators, present a irreducible hadronic ambiguity from the viewpoint of this analysis.

Empirical information on the all-neutral mode, a_{00}, is essential to the extraction of α; however, it is possible to bound the strong-phase uncertainty using bounds on a_{00} and its CP-conjugate $\overline{a}_{00}$ [19]. Under the assumptions we have articulated, the bounds on the hadronic uncertainty realized in $B\to\rho\pi$ decay [19] are not modified by the presence of a $|\Delta I|=5/2$ transition.

An isospin analysis of $B\to\pi\pi$ decay also permits the extraction of $\sin(2\alpha)$ from the mixing-induced CP asymmetry in $B\to\pi^+\pi^-$ [32]. In this case, in contrast, the $|\Delta I|=5/2$ amplitude cannot be combined with the $|\Delta I|=3/2$ amplitude. With $A_{|\Delta I|,I_f}$, we have

$$b_{+-}\equiv A(B^0\to\pi^+\pi^-)=-\frac{1}{\sqrt{3}}A_{1/2,0}+\frac{1}{\sqrt{6}}[A_{3/2,2}-A_{5/2,2}], \tag{10}$$

$$b_{00}\equiv A(B^0\to\pi^0\pi^0)=-\frac{1}{\sqrt{3}}A_{1/2,0}-\sqrt{\frac{2}{3}}[A_{3/2,2}-A_{5/2,2}], \tag{11}$$

$$b_{+0}\equiv A(B^+\to\pi^+\pi^0)=\frac{\sqrt{3}}{2}A_{3/2,2}+\frac{1}{\sqrt{2}}A_{5/2,2}. \tag{12}$$

As the case of $B\to\rho\pi$, three isospin amplitudes describe three empirical amplitudes, so that we expect our parametrization to persist in the presence of isospin violation. The lowest-dimension operators of the effective weak Hamiltonian generate transitions of $|\Delta I|=1/2$ and $|\Delta I|=3/2$ character, so that in the absence of isospin-violating effects in the hadronic matrix elements, $A_{1/2,0}\to A_0$ and $A_{3/2,2}\to A_2$, and two amplitudes suffice to describe the three transitions. The isospin analysis in $B\to\pi\pi$ relies on the relation $(b_{+-}-b_{00})/\sqrt{2}-b_{+0}=0$ [32]. The right-hand side of this relation is proportional to $A_{5/2,2}$, so that the required relation is broken by amplitudes of $|\Delta I|=5/2$ character. With such effects the isospin analysis can fail to determine the true value of $\sin(2\alpha)$ [25]. The small $B\to\pi^0\pi^0$ rate makes the full isospin analysis difficult to effect, so that bounds on the hadronic uncertainty in the extraction of $\sin(2\alpha)$ have also been constructed [33–36]. The presence of the $|\Delta I|=5/2$ amplitude, as well as that of electroweak penguins, imply that the bounds can underestimate the size of the hadronic uncertainty [25]. However, bounds which rely on the neutral B modes exclusively, such as Eq. (83) of Ref. [33], contain the same linear combination of $|\Delta I|=3/2$ and $|\Delta I|=5/2$ amplitudes throughout—so that our arguments concerning the $|\Delta I|=5/2$ amplitude in $B\to\rho\pi$ decay are germane here as well. We conclude, to the extent the $|\Delta I|=3/2$ and $|\Delta I|=5/2$ amplitudes share the same weak phase, that such bounds are insensitive to the $|\Delta I|=5/2$ amplitude and yield more reliable bounds on the hadronic uncertainty.

III. EXTENSION OF THE ISOSPIN ANALYSIS: INCLUSION OF THE $\sigma\pi$ CHANNEL

The $B\to\sigma\pi$ channel has definite properties under CP, so that it can be included in the $B\to\rho\pi$ analysis as well. Defining $a_{00}^{\sigma}=A(B^0\to\sigma\pi^0)$, we have

$$e^{i\beta}a_{00}^{\sigma}=T_{\sigma}^{00}e^{-i\alpha}+P_{\sigma}^{00}. \tag{13}$$

T_{σ}^{00} and P_{σ}^{00} are unrelated to the parameters of Eq. (8), so that we gain four additional hadronic parameters. However, more observables are present as well. Including the scalar channel, we now have $A_{3\pi}\equiv A(B^0\to\pi^+\pi^-\pi^0)=f_+\,a_{+-}+f_-\,a_{-+}+f_0\,a_{00}+f_\sigma\,a_{00}^{\sigma}$, where f_σ is the form factor describing $\sigma\to\pi^+\pi^-$. It is worth noting that any discernable presence of the $B\to\sigma\pi$ channel in the $B\to\rho\pi$ phase space falsifies the notion that the ''nonresonant'' background can be characterized by a single, constant phase across the Dalitz plot [37]. For further discussion of the treatment of nonresonant contributions, specifically in $D\to3\pi$ decay, see Ref. [38]—note also Ref. [7].

Neglecting the width difference of the B-meson mass eigenstates, as $\Delta\Gamma\equiv\Gamma_H-\Gamma_L$ and $|\Delta\Gamma|\ll\Gamma\equiv(\Gamma_H+\Gamma_L)/2$, we note that the decay rate into $\pi^+\pi^-\pi^0$ for a B^0 meson at time $t=0$ is given by [39]

$$\Gamma(B^0(t)\to\pi^+\pi^-\pi^0)=|A_{3\pi}|^2\exp(-\Gamma t)\left[\frac{1+|\lambda_{3\pi}|^2}{2}+\frac{(1-|\lambda_{3\pi}|^2)}{2}\cos(\Delta m\,t)-\mathrm{Im}\,\lambda_{3\pi}\sin(\Delta m\,t)\right], \tag{14}$$

whereas the decay rate into $\pi^+\pi^-\pi^0$ for a $\overline{B}^0$ meson at time $t=0$ is given

$$\Gamma(\overline{B}^0(t)\to\pi^+\pi^-\pi^0)=|A_{3\pi}|^2\exp(-\Gamma t)\left[\frac{1+|\lambda_{3\pi}|^2}{2}-\frac{(1-|\lambda_{3\pi}|^2)}{2}\cos(\Delta m\,t)+\mathrm{Im}\,\lambda_{3\pi}\sin(\Delta m\,t)\right]. \tag{15}$$

We note that $\lambda_{3\pi}\equiv q\overline{A}_{3\pi}/pA_{3\pi}$, where we have defined $\overline{A}_{3\pi}\equiv A(\overline{B}^0\to\pi^+\pi^-\pi^0)$, and $\Delta m\equiv M_H-M_L$. Different observables are possible. For example, we can consider untagged observables, for which the identity of the B meson at $t=0$ is unimportant, so that $\Gamma(B^0(t)\to\pi^+\pi^-\pi^0)+\Gamma(\overline{B}^0(t)\to\pi^+\pi^-\pi^0)\propto(1+|\lambda_{3\pi}|^2)$, or we can consider time-integrated, tagged observables, containing $\Gamma(B^0(t)\to\pi^+\pi^-\pi^0)-\Gamma(\overline{B}^0(t)\to\pi^+\pi^-\pi^0)$, which are sensitive to $(1-|\lambda_{3\pi}|^2)$. The products $f_if_j^*$ contained therein are distinguishable through the Dalitz plot of this decay and thus the coefficients of these functions are distinct observables [6]. Were we to neglect the $\sigma\pi$ channel, nine distinct, untagged observables exist, so that all the hadronic parameters save one would be determinable from the untagged data, for which greater statistics will be available [19]. If we enlarge the analysis to include the $\sigma\pi^0$ channel, the additional interferences possible imply that there are now sixteen distinct, untagged observables. Moreover, there are fifteen, rather than eight, tagged, time-integrated observables as well. Nevertheless, it would seem that the additional hadronic parameters associated with the $\sigma\pi^0$ final state can be extracted from untagged data alone. Of course the practicability of the procedure relies on the amount of data eventually collected; moreover, the observables are highly correlated.

IV. EVALUATING $B\to\pi^+\pi^-\pi^0$ DECAY

The effective, $|\Delta B|=1$ Hamiltonian for $b\to dq\overline{q}$ decay is given by

$$\mathcal{H}_{\mathrm{eff}}=\frac{G_F}{\sqrt{2}}\left[\lambda_u(C_1O_1^u+C_2O_2^u)+\lambda_c(C_1O_1^c+C_2O_2^c)-\lambda_t\sum_{i=3}^{10}C_iO_i\right], \tag{16}$$

where $\lambda_q \equiv V_{qb}V_{qd}^*$ with V_{ij} an element of the CKM matrix. The Wilson coefficients C_i and operators O_i are detailed in Ref. [40], though we shall interchange $C_1 O_1^q \leftrightarrow C_2 O_2^q$ so that $C_1 \sim \mathcal{O}(1)$ and $C_1 > C_2 \gg C_{3\ldots10}$. The contributions with $i=3\ldots6$ correspond to strong penguin effects, whereas those with $i=7\ldots10$ are characterized by electroweak penguin effects. The Wilson coefficients with $i=7\ldots10$ are numerically smaller than those with $i=3\ldots6$, and penguin effects are not CKM-enhanced in $b\to dq\bar{q}$ decay, so that we shall neglect the terms with $i=7\ldots10$ all together.

The decay amplitude for $B\to M_1M_2$, where M_1 and M_2 are mesons, is given by

$$A(B\to M_1M_2)=\langle M_1M_2|\mathcal{H}_{\rm eff}|B\rangle. \tag{17}$$

The requisite matrix element contains terms of the form

$$C_i(\mu)\langle M_1M_2|O_i|B\rangle. \tag{18}$$

We adopt the naive factorization approximation to effect estimates of the hadronic matrix elements. To wit, we separate O_i into a product of factorized currents, $j_1\otimes j_2$, and evaluate $\langle M_1|j_1|B\rangle\langle M_2|j_2|0\rangle$, so that the operator matrix element becomes a product of a form factor and a decay constant. Such a treatment, albeit simple, is incomplete. The amplitude $A(B\to M_1M_2)$ is related to a physical observable and as such must be μ-independent, though the C_i therein do depend on μ. Evidently the μ dependence of the operator matrix elements compensates to yield a μ independent result. In the naive factorization approximation, we have replaced the operator matrix element by a product of a form factor and decay constant. These quantities are themselves physical observables and thus are without μ dependence, so that the overall μ dependence of the computed amplitude remains. Effecting this approximation, however, allows us to realize a clear connection to earlier work [9,16], for our purpose is to illustrate the impact of using a scalar form factor consistent with low-energy constraints.

In the naive factorization approximation, we can replace the effective Hamiltonian by the sum of products of factorized currents, so that $\mathcal{H}_{\rm eff}=\mathcal{T}^{1,2}+\mathcal{T}^{3,4}+\mathcal{T}^{5,6}$, where

$$\mathcal{T}^{1,2}=\frac{G_F}{\sqrt{2}}\lambda_u\left[a_1\bar{u}\gamma^\mu(1-\gamma_5)b\otimes\bar{d}\gamma_\mu(1-\gamma_5)u + a_2\bar{d}\gamma^\mu(1-\gamma_5)b\otimes\bar{u}\gamma_\mu(1-\gamma_5)u\right], \tag{19}$$

$$\mathcal{T}^{3,4}=-\frac{G_F}{\sqrt{2}}\lambda_t\left[a_3\sum_q\ \bar{d}\gamma^\mu(1-\gamma_5)b\otimes\bar{q}\gamma_\mu(1-\gamma_5)q + a_4\sum_q\ \bar{q}\gamma^\mu(1-\gamma_5)b\otimes\bar{d}\gamma_\mu(1-\gamma_5)q\right], \tag{20}$$

and

$$\mathcal{T}^{5,6}=-\frac{G_F}{\sqrt{2}}\lambda_t\left[a_5\sum_q\ \bar{d}\gamma^\mu(1-\gamma_5)b\otimes\bar{q}\gamma_\mu(1+\gamma_5)q - 2a_6\sum_q\ \bar{q}(1-\gamma_5)b\otimes\bar{d}(1+\gamma_5)q\right]. \tag{21}$$

We define $a_i\equiv C_i+C_{i+1}/3$ for i odd and $a_i\equiv C_i+C_{i-1}/3$ for i even; note, too, that $q\in u,d,s,c$ if $\mu\lesssim m_b$.

We now specifically consider $B\to\sigma\pi$ transitions; the relevant formulas for $B\to\rho\pi$ are detailed in the Appendix. By "σ," we always mean a two-pion state with total isospin zero and in a relative S-wave state, $(\pi\pi)_S$, understanding its dynamical origin in the strong pionic FSI for these quantum numbers—see the following section for a more detailed discussion. The matrix elements involving the σ are

$$q^\mu\langle\sigma(p_\sigma)|\bar{d}\gamma_\mu(1-\gamma_5)b|\bar{B}^0(p_B)\rangle = -i(M_B^2-M_\sigma^2)F_0^{B\to\sigma}(q^2), \tag{22}$$

where $q\equiv p_B-p_\sigma$ and $\langle\sigma|\bar{q'}\gamma_\mu(1+\gamma_5)q'|0\rangle$, noting $q'\in u,d,s$, *vanishes* by C invariance. It is just such a suppression mechanism that prompts the authors of Ref. [41] to argue that non-factorizable effects ought be relatively enhanced in two-body B decays to final states with scalar mesons, as the factorization contribution is itself small. Nevertheless, as our focus is the scalar form factor itself, we proceed with our estimates.

For the π^+ we have

$$\langle\pi^+(p)|\bar{u}\gamma^\mu(1-\gamma_5)d|0\rangle=if_\pi p^\mu \tag{23}$$

and

$$\langle\pi^+(p)|\bar{u}\gamma_\mu(1-\gamma_5)b|\bar{B}^0(p_B)\rangle = \left[(p_B+p)_\mu-\frac{(M_B^2-M_\pi^2)}{q^2}q_\mu\right]F_1^{B\to\pi}(q^2) + \frac{(M_B^2-M_\pi^2)}{q^2}q_\mu F_0^{B\to\pi}(q^2). \tag{24}$$

With these relations, Eqs. (19), (20), (21), and the equations of motion for the quark fields, we have

$$\langle\pi^-\sigma|\mathcal{H}_{\rm eff}|B^-\rangle = \frac{G_F}{\sqrt{2}}\left\{f_\pi(M_B^2-M_\sigma^2)F_0^{B\to\sigma}(M_\pi^2) \times\left[\lambda_u a_1-\lambda_t a_4+\lambda_t\frac{a_6M_\pi^2}{\hat{m}(m_b+\hat{m})}\right] + \lambda_t 2a_6\frac{\langle\sigma|\bar{d}d|0\rangle}{(m_b-\hat{m})}(M_B^2-M_\pi^2)F_0^{B\to\pi}(M_\sigma^2)\right\} \tag{25}$$

and

$$\langle \pi^0\sigma|\mathcal{H}_{\rm eff}|\bar{B}^0\rangle = \frac{G_F}{\sqrt{2}}\left\{ \frac{f_\pi}{\sqrt{2}}(M_B^2 - M_\sigma^2)F_0^{B\to\sigma}(M_\pi^2) \times\left[\lambda_u a_2 + \lambda_t a_4 - \lambda_t \frac{a_6 M_\pi^2}{\hat{m}(m_b+\hat{m})}\right] - \lambda_t 2a_6 \frac{\langle\sigma|\bar{d}d|0\rangle}{(m_b-\hat{m})}(M_B^2 - M_\pi^2) \times\frac{F_0^{B\to\pi}(M_\sigma^2)}{\sqrt{2}}\right\}, \tag{26}$$

where we have replaced the u,d quark masses with $\hat{m}$ and set $M_{\pi^0}=M_{\pi^\pm}=M_\pi$ and $M_{B^\pm}=M_{B^0,\bar{B}^0}=M_B$, as we neglect isospin-violating effects. We adopt the usual phase conventions for the flavor wave functions $\pi^+,\pi^0,\pi^- = u\bar{d},(u\bar{u}-d\bar{d})/\sqrt{2},d\bar{u}$, and adopt analogous relations for the ρ mesons as well. In the context of the $B\to\rho\pi$ analysis, the decay $\bar{B}^0\to\sigma\pi$, specifically its penguin contributions, modify Eq. (9), the assumption crucial to the analysis. Thus it is important to make an assessment of the size of penguin effects in this decay. The terms containing a_6, the scalar penguin contribution, are formally $1/m_b$ suppressed, but can be chirally enhanced: the numerical factor $M_\pi^2/(\hat{m}m_b)\sim 0.6$ is only modestly less than unity. The second term proportional to a_6 contains $\langle\sigma|\bar{d}d|0\rangle$, where we anticipate, in the vicinity of the σ resonance, $\Gamma_{\sigma\pi\pi}(s)\langle\sigma|\bar{d}d|0\rangle = \langle\pi^+(p_+)\pi^-(p_-)|\bar{d}d|0\rangle = \sqrt{2/3}B_0\Gamma_1^n{}^*(s)$, where $\Gamma_1^n(s)$ is the scalar form factor, which we detail in the next section, and $s=(p_+ + p_-)^2$. The parameter B_0 is related to the vacuum quark condensate. Neglecting small terms of second order in the quark masses, $B_0 = -\langle 0|\bar{q}q|0\rangle/F_\pi^2$, where F_π, the π^0 decay constant, is $f_\pi/\sqrt{2}$. Commensurately, we can simply set $B_0 \equiv M_\pi^2/(2\hat{m})$ to realize our numerical estimates. Note that $\Gamma_{\sigma\pi\pi}$ describes the $\sigma\to\pi^+\pi^-$ form factor. With our conventions, $B_0>0$, so that the two a_6 contributions are of the same sign. Using the parameters of Ref. [9] and $\Gamma_{\sigma\pi\pi}=\Gamma_1^n{}^*\chi$ with, as we shall determine, $\chi = 20.0\ \text{GeV}^{-1}$, we find the a_6 term containing f_π to be roughly a factor of four larger. The $\langle\sigma|\bar{d}d|0\rangle$ term, present in the penguin contributions in $B\to\sigma\pi$, slightly enhances the a_6 contribution and its subsequent cancellation with the a_4 contribution, as a_4 and a_6 are of the same sign. The same cancellation occurs in $\bar{B}^0\to\rho^0\pi^0$ (see the Appendix for a compilation of the relevant formulas), so that penguin contributions in $\bar{B}^0\to\sigma\pi^0$ can be expected to be crudely comparable to those in $\bar{B}^0\to\rho^0\pi^0$. Modifications of Eq. (9) can thus be expected to occur.

In the previous section we determined how the isospin analysis in $B\to\rho\pi$ could be extended to include $B\to\sigma\pi$. Equations (25) and (26), however, are related by isospin symmetry, so that it is useful to determine whether additional constraints on P_σ^{00} in Eq. (13) can be realized. Parametrizing the amplitudes in terms of $A_{|\Delta I|,I_f}$, we have

$$A(B^0\to\sigma\pi^0) = \frac{1}{\sqrt{2}}A_{1/2,1} - \frac{1}{\sqrt{2}}A_{3/2,1} \tag{27}$$

and

$$A(B^+\to\sigma\pi^+) = -A_{1/2,1} - \frac{1}{2}A_{3/2,1}, \tag{28}$$

so that two isospin amplitudes appear for the two empirical amplitudes. Although the $|\Delta I|=1/2$ amplitudes are simply related, we see that no useful constraint emerges, as the tree amplitude in $B^+\to\sigma\pi^+$, which includes $|\Delta I|=1/2$ and 3/2 amplitudes, gives rise to two additional, undetermined hadronic parameters.

We have illustrated that the penguin relation essential to the isospin analysis in $B\to\rho\pi$, Eq. (9), can be broken through the presence of the $B\to\sigma\pi$ decay channel. In our numerical estimates, however, we neglect penguin contributions, in order to retain a crisp comparison with earlier work [9], for our purpose is to illuminate the impact of the $\sigma\to\pi^+\pi^-$ form factor. With such an approximation, a computation of the Wilson coefficients in leading order in α_s suffices [42], so that $C_1(\mu)=1.124$ and $C_2(\mu)=-0.271$ at $\mu=m_b=4.8$ GeV as per Ref. [43], to yield $a_1=1.034$ and $a_2=0.104$. In contrast, Ref. [9] uses the ''fitted'' values $C_1(m_b)=1.105$ and $C_2(m_b)=-0.228$, to yield $a_1=1.029$ and $a_2=0.140$. These are very similar to the Wilson coefficients in next-to-leading-order QCD, after Ref. [44], used in the $B\to\rho\pi$ analysis of Ref. [16]. For definiteness, we shall adopt these last values, detailed in Sec. VII, in our numerical analysis. The values of a_1 are quite similar, whereas those of a_2 differ by tens of percent. Generally, we expect our numerical predictions for decay channels controlled by a_2 to be less robust, as the scale dependence of a_2, as illustrated in Table III of Ref. [43], is severe. Note that it persists to a significant degree in the next-to-leading order treatment of Ref. [30] as well.

Nevertheless, let us proceed to consider numerical estimates for $B\to\sigma\pi$ decay. We reconstruct the σ meson from the $(\pi^+\pi^-)_S$ final state, so that we have

$$A_\sigma(B\to\pi^+\pi^-\pi) \equiv \langle(\sigma\to\pi^+\pi^-)\pi|\mathcal{H}_{\rm eff}|B\rangle = A(B\to\sigma\pi)\Gamma_{\sigma\pi\pi}, \tag{29}$$

where $\Gamma_{\sigma\pi\pi}$ is the $\sigma\to\pi^+\pi^-$ form factor introduced previously. The scalar form factor contains the meson loop function and thus a regularization scale μ_r at which it is evaluated. In our approach, this scale dependence is disjoint from that associated with the renormalization of the operators of the effective, weak Hamiltonian, so that it is chosen for convenience and is quite independent of μ. It may seem untoward to graft two very different calculations, namely, of $A(B\to\sigma\pi)$ and of $\Gamma_{\sigma\pi\pi}$, to yield $A(B\to(\sigma\to\pi^+\pi^-)\pi)$. In a holistic treatment one might hope to recast a resonance and its subsequent decay products in terms of a single, com-

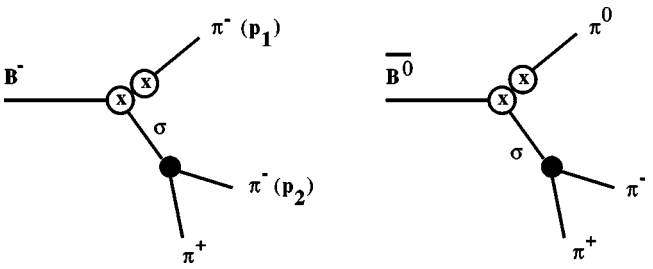

FIG. 1. $B\to\pi^+\pi^-\pi$ decay as mediated by the σ resonance. The factorized weak vertex is denoted by ''$\otimes\otimes$.'' The filled circle denotes the strong three-meson vertex, here $\sigma\to 2\pi$.

plex hadron distribution amplitude, $\phi(x,\mu)$, which describes the non-perturbative dynamics. The analysis of the decay amplitude could then proceed via standard PQCD techniques [45,46]. In this manner the μ_r dependence of which we have spoken is connected, albeit loosely, to the scale dependence of $\phi(x,\mu)$. Nevertheless, the explicit ''QCD factorization'' analysis of Ref. [30] shows that the scale dependence of the hadron distribution functions is trivial in an NLO analysis in α_s, so that the consistency issues to which we have alluded are beyond the scope of current calculations.

Turning to $B^-(p_B)\to\pi^+(p_+)\pi^-(p_1)\pi^-(p_2)$ decay, we define $u=(p_B-p_1)^2=(p_++p_2)^2$ and $t=(p_++p_1)^2$. The contributions driven by the σ resonance are of the form $B^-(p_B)\to(\sigma\to\pi^+(p_+)\pi^-(p_1))\pi^-(p_2)$ or $B^-(p_B)\to(\sigma\to\pi^+(p_+)\pi^-(p_2))\pi^-(p_1)$—the latter is illustrated in Fig. 1. (The corresponding contributions to $B\to\rho\pi$ decay are illustrated in Fig. 2.) The two contributions add coherently, so that the branching ratio for $B^-(p_B)\to\pi^+(p_+)\pi^-(p_1)\pi^-(p_2)$ is enhanced through the presence of two identical pions in the final state. In $\overline{B}^0$ decay this does not occur, and we have $\overline{B}^0(p_B)\to\pi^+(p_+)\pi^-(p_1)\pi^0(p_2)$. Thus we find

$$\langle(\sigma\to\pi^+\pi^-)\pi^-|\mathcal{H}_{\rm eff}|B^-\rangle = \frac{G_F}{\sqrt{2}}V_{ub}^*V_{ud}\,a_1\,F_0^{(B\to\sigma)}(M_\pi^2)(M_B^2-M_\sigma^2) \times f_\pi[\Gamma_{\sigma\pi\pi}(t)+\Gamma_{\sigma\pi\pi}(u)], \tag{30}$$

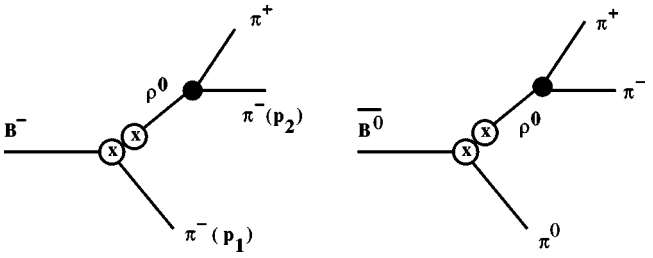

FIG. 2. $B\to\pi^+\pi^-\pi$ decay as mediated by the ρ resonance. The factorized weak vertex is denoted by ''$\otimes\otimes$.'' The filled circle denotes the strong three-meson vertex, here $\rho\to 2\pi$.

$$\langle(\sigma\to\pi^+\pi^-)\pi^0|\mathcal{H}_{\rm eff}|\overline{B}^0\rangle = \frac{G_F}{\sqrt{2}}V_{ub}^*V_{ud}\,a_2\,F_0^{(B\to\sigma)}(M_\pi^2)(M_B^2-M_\sigma^2) \times\frac{f_\pi}{\sqrt{2}}\Gamma_{\sigma\pi\pi}(t). \tag{31}$$

In Ref. [9], the $\sigma\to\pi^+\pi^-$ vertex function is chosen to be

$$\Gamma_{\sigma\pi\pi}(x)=g_{\sigma\pi^+\pi^-}\left(\frac{1}{x-M_\sigma^2+i\Gamma_\sigma(x)M_\sigma}\right), \tag{32}$$

where the running width $\Gamma_\sigma(x)$ is defined as

$$\Gamma_\sigma(x)=\Gamma_\sigma\frac{M_\sigma}{\sqrt{x}}\frac{\sqrt{x/4-M_\pi^2}}{\sqrt{M_\sigma^2/4-M_\pi^2}}. \tag{33}$$

We shall adopt, however, the definition

$$\Gamma_{\sigma\pi\pi}(x)=\chi\,\Gamma_1^n{}^*(x), \tag{34}$$

where the normalization χ is fixed to be identical to that of Eq. (32), namely

$$\chi|\Gamma_1^n(M_\sigma^2)|=\frac{g_{\sigma\pi^+\pi^-}}{\Gamma_\sigma(M_\sigma^2)M_\sigma}. \tag{35}$$

Using the parameters $g_{\sigma\pi^+\pi^-}$, M_σ, and Γ_σ of Ref. [9], that is, $M_\sigma=478\pm 24$ MeV and $\Gamma_\sigma=324\pm 41$ MeV as reported by the E791 Collaboration in $D^+\to 3\pi$, and $g_{\sigma\pi\pi}=2.52$ GeV, we find $\chi=20.0$ GeV^{-1}. Alternatively, $\chi=\sqrt{2/3}B_0/\langle\sigma|\bar{d}d|0\rangle$, so that this procedure determines $\langle\sigma|\bar{d}d|0\rangle$ as well.

The σ meson is a broad $I=J=0$ enhancement, close to the ρ meson in mass, so that $B\to\sigma\pi$ decay can contribute to the allowed phase space of $B\to\rho\pi$ decay as well. To ascertain the impact of the $B\to\sigma\pi$ channel to $B\to\rho\pi$ decay, we combine the decay channels at the amplitude level and then integrate over the relevant three-body phase space to determine the *effective* $B\to\rho\pi$ branching ratio. For $B(p_B)\to\pi^+(p_+)\pi^-(p_1)\pi(p_2)$ decay, we define

$$\cos\theta=\frac{\mathbf{p}_1'\cdot\mathbf{p}_2'}{|\mathbf{p}_1'||\mathbf{p}_2'|}, \tag{36}$$

where the primed variables refer to the momenta in the rest frame of the $\pi^+(p_+')\pi^-(p_1')$ pair, so that $\mathbf{p}_1'+\mathbf{p}_+'=0$. Letting $p_2^2=M_2^2$, we have

$$\Gamma(B\to\rho_{\rm eff}\pi)=\int_{-1}^{1}d\cos\theta\int_{(M_\rho-\delta)^2}^{(M_\rho+\delta)^2}dt\frac{1}{32(4\pi M_B)^3} \times(M_B^2-t-M_2^2)\beta_1'\beta_2'|\mathcal{M}|^2, \tag{37}$$

where "$\rho_{\rm eff}$" is determined by $(M_\rho-\delta)^2 \leqslant t \leqslant (M_\rho+\delta)^2$, β_i' refers to the velocity of particle i in the primed frame, and $\mathcal{M}$ is the sum of the amplitudes of interest.[3] Typically $\delta \sim (1-2)\Gamma_\rho$.

The scalar form factor we adopt describes the $f_0(980) \to \pi^+\pi^-$ vertex function as well, albeit with a new normalization factor, as

$$\Gamma_{f_0\pi\pi}(t)\langle f_0|\bar{d}d|0\rangle = \langle \pi^+(p_+)\pi^-(p_1)|\bar{d}d|0\rangle = \sqrt{2/3}B_0\Gamma_1^{n\,*}(t),$$

in the vicinity of the $f_0(980)$ resonance. The appearance of the $f_0(980)$ resonance in the $\pi^+\pi^-$ channel is complicated by the opening of the $K\bar{K}$ threshold; the $f_0(980)\to\pi^+\pi^-$ form factor is decidedly not of Breit-Wigner form. It should be noted that the unitarization procedure we employ here neglects the $\eta\eta$ channel, though, as we discuss in the next section, this has no impact on the description of $\pi\pi$ scattering below $s\simeq 1.1$ GeV. Note, too, that although multiparticle final states, particularly the 4π state, can contribute, they are demonstrably small for $s\leqslant 1.4$ GeV [47,48]. The form factor(s) we adopt can be tested though the *shape* of the $f_0(980)$ contribution in $B\to f_0(980)\pi\to 3\pi$, as well as through that in $B\to f_0(980)\pi\to K^+K^-\pi$.

V. COUPLED-CHANNEL PION AND KAON SCALAR FORM FACTORS

In the preceding section, we encountered the non-strange, scalar form factor of the pion, $\Gamma_1^n(t)$. Such scalar form factors play a unique role in strong-interaction physics because they measure the strength of the quark mass term $\mathcal{H}_m^{\rm QCD} = m_u\bar{u}u + m_d\bar{d}d + \cdots$, i.e., the explicit chiral-symmetry-breaking term in QCD. However, since no scalar-isoscalar sources exist, these form factors cannot be determined directly but, rather, must be inferred indirectly from hadron-hadron scattering data. The most prominent example in this context is the pion-nucleon sigma term, which can be extracted from the analytically-continued and Born-term-subtracted isoscalar S-wave amplitude. Similarly, the pion scalar form factor can be obtained from meson-meson scattering data, with the added complication of channel couplings above the $\bar{K}K$ threshold at $\sqrt{s}\simeq 1$ GeV. At lower energies, the pion scalar form factor can be calculated in CHPT at one- [49] and two-loop accuracy [50,51]. The one-loop representation fails at surprisingly low energies, a consequence of the strong pionic FSI present in this channel [52]. This is also signaled by the very large pion scalar radius, $\langle r_S^2\rangle_\pi \simeq 0.6$ fm^2, which is sizeably bigger than the pion vector radius governed by the rho mass $\langle r_V^2\rangle_\pi \simeq 6/M_\rho^2 \simeq 0.4$ fm^2, indicating a smaller breakdown scale in the scalar-isoscalar channel. In fact, these FSI are so strong that they can dynamically generate the σ meson, with no need of a genuine (pre-existing) quark model state [53]. Furthermore, extending such an analysis to three flavors, one finds that all the scalar mesons with mass below 1.1 GeV can be dynamically generated, so that the genuine quark model nonet would have its center of gravity at about 1.3 GeV, see e.g. Ref. [54] and references therein. Irrespective of this admittedly controversial assignment of the scalars, for further recent discussion see Ref. [55], the pion scalar form factor *cannot* be represented simply in terms of a scalar meson with a certain mass and width. Although the *description* of the low-lying scalar states in terms of dynamically generated, rather than "pre-existing," states may be controversial and thus subject to ongoing discussion, let us stress that the scalar form factor itself is not. The form factor which emerges for the chiral unitary approach adopted here is quite comparable to that which emerges from the dispersion analysis of Ref. [56]. Consequently, when one has a source with vacuum quantum numbers coupled to a two-pion state, it can be very misleading to use a simple Breit-Wigner parametrization, albeit with a running width. We shall display this graphically after discussing the scalar form factor and its construction, to be used in calculating the branching ratios to which we have alluded. We note in passing that this casts doubt on the extraction of the σ meson properties from $D\to 3\pi$ decays, note Ref. [8]. This is quite in contrast to the pion vector form factor and the ρ meson, for which such a description works to good accuracy.

We now summarize how to calculate the scalar form factor in Eq. (34), following Ref. [10], to which we refer in all details. Of course, one could also use the numerical result of the dispersion analysis of [56] for the scalar form factor. Note that the band found there overlaps with the band of Ref. [10] if one allows for parameter variations within known bounds. As a first step, we prefer to work in the framework of the chiral unitary approach, as it yields a form factor which is more convenient for applications. As we have noted, we need the scalar form factor of the pion for momentum transfers larger than 1 GeV. Consequently, we cannot work with the scalar form factor as computed in CHPT, but must invoke some resummation technique, as well as account for the channel coupling between the $\pi\pi$ and the $K\bar{K}$ systems. The resummation method is constrained only by unitarity and thus is not entirely model-independent. However, it can be strongly constrained by requiring that the so-constructed form factors match the CHPT expressions, in the region where CHPT is applicable. Due to the channel coupling, we have to consider transition matrix elements of the nonstrange and strange scalar quark bilinears between two meson states of isospin zero, namely $\pi\pi$ and $\bar{K}K$, and the vacuum. We exclude the $\eta\eta$ channel, as it does not affect the phase shifts or pion-kaon decays and transitions—it only plays a role in describing the inelasticity of $I=J=0$ $\pi\pi$ scattering above 1.1 GeV, the physical $\eta\eta$ threshold. For a detailed discussion of this point, we refer to Refs. [53,57,58]. The pertinent matrix elements are given in terms of four

[3]For completeness, we note that $u = M_+^2 + M_2^2 + 2E_+'E_2'(1 + \beta_1'\beta_2'\cos\theta)$, with $E_+' = (t + M_+^2 - M_1^2)/(2\sqrt{t})$, $E_1' = (t + M_1^2 - M_+^2)/(2\sqrt{t})$, and $E_2' = (M_B^2 - t - M_2^2)/(2\sqrt{t})$, where $p_+^2 = M_+^2$ and $p_1^2 = M_1^2$.

scalar form factors,[4]

$$\langle 0|\overline{nn}|\pi\pi\rangle=\sqrt{2}\,B_0\,\Gamma_1^n(s),\qquad \langle 0|\overline{nn}|K\overline{K}\rangle=\sqrt{2}\,B_0\,\Gamma_2^n(s),$$
$$\langle 0|\overline{ss}|\pi\pi\rangle=\sqrt{2}B_0\,\Gamma_1^s(s),\qquad \langle 0|\overline{ss}|K\overline{K}\rangle=\sqrt{2}\,B_0\,\Gamma_2^s(s), \tag{38}$$

where B_0 is a measure of the vacuum quark condensate, $B_0=-\langle 0|\overline{qq}|0\rangle/F_\pi^2$, with $F_\pi\simeq 93$ MeV the pion decay constant (strictly speaking its value in the limit of vanishing quark masses). In Eq. (38), the following notation is employed. The superscript $s(n)$ refers to the strange-nonstrange quark operator whereas the subscript $1(2)$ denotes pions and kaons, respectively. Furthermore, $\overline{nn}=(\overline{uu}+\overline{dd})/\sqrt{2}$. The pion scalar form factors $\Gamma_1^n(s)$ and $\Gamma_1^s(s)$ are calculated in Refs. [49,59] through one loop in CHPT and $\Gamma_1^n(s)$ through two loops in Refs. [50,51]. The scalar kaon form factors at next-to-leading order in CHPT were first explicitly given in Ref. [10]. Since it is central to our discussion, we give the explicit expression for $\Gamma_1^n(s)$ [59]

$$\Gamma_1^n(s)=\sqrt{\frac{3}{2}}\Bigg\{1+\mu_\pi-\frac{1}{3}\mu_\eta+\frac{16M_\pi^2}{F_\pi^2}(2L_8^r-L_5^r)+8(2L_6^r-L_4^r)\frac{2M_K^2+3M_\pi^2}{F_\pi^2}+f(s)+\frac{2}{3}\tilde{f}(s)\Bigg\}, \tag{39}$$

with $f(s)$ and $\tilde{f}(s)$ given by

$$f(s)=\frac{2s-M_\pi^2}{2F_\pi^2}\overline{J}_{\pi\pi}(s)-\frac{s}{4F_\pi^2}\overline{J}_{KK}(s)-\frac{M_\pi^2}{6F_\pi^2}\overline{J}_{\eta\eta}(s)+\frac{4s}{F_\pi^2}\Bigg\{L_5^r-\frac{1}{256\pi^2}\Bigg(4\log\frac{M_\pi^2}{\mu^2}-\log\frac{M_K^2}{\mu^2}+3\Bigg)\Bigg\},$$

$$\tilde{f}(s)=\frac{3}{4}\frac{s}{F_\pi^2}\overline{J}_{KK}(s)+\frac{M_\pi^2}{3F_\pi^2}\overline{J}_{\eta\eta}(s)+\frac{12s}{F_\pi^2}\Bigg\{L_4^r-\frac{1}{256\pi^2}\times\Bigg(\log\frac{M_K^2}{\mu^2}+1\Bigg)\Bigg\}. \tag{40}$$

Here, $\overline{J}_{PP}(s)$ $(P=\pi,K,\eta)$ is the standard meson loop function [49], and μ, in this section, is the scale of dimensional regularization. The quantities μ_P in Eq. (39) are given by

$$\mu_P=\frac{m_P^2}{32\pi^2F_\pi^2}\log\frac{m_P^2}{\mu^2}. \tag{41}$$

[4]Here "$\pi\pi$" and "KK" states denote the linear combinations of physical $\pi\pi$ and KK states, respectively, with zero total isospin.

Furthermore, the $L_i^r(\mu)$ are scale-dependent, renormalized low-energy constants. We use here the same values as in Ref. [10]. Since the combination $2L_6^r-L_4^r$ multiplies M_K^2, the normalization of $\Gamma_1^n(s)$ is sensitive to the precise value of these low-energy constants, which are only poorly known. This motivates our choice for the normalization of $\Gamma_{\sigma\pi\pi}(s)$, given in Eq. (35). The one-loop representation cannot be trusted beyond $\sqrt{s}\simeq 400$ MeV, as it begins to diverge from the form factor extracted from $\pi\pi$ scattering data. To go to higher energies, one therefore has to study the constraints that unitarity imposes on the scalar form factors. The imaginary part of any scalar form factor is given by the appropriate meson-meson scattering T-matrix, so that the starting point for any unitary resummation scheme is exactly this scattering T-matrix [60],

$$T(s)=[I+K(s)\cdot g(s)]^{-1}\cdot K(s), \tag{42}$$

where s denotes the center-of-mass energy squared and $K(s)$ can be obtained from the lowest order CHPT Lagrangian, e.g., $K(s)_{11}=(s-M_\pi^2/2)/F_\pi^2$. This T-matrix not only describes meson-meson scattering data but also, after gauging, photon decays and transitions, as reviewed in Ref. [11]. In Eq. (42), the diagonal matrix $g(s)$ is nothing but the familiar scalar loop integral

$$g(s)_i=\frac{1}{(4\pi)^2}\Bigg(-1+\log\frac{M_i^2}{\mu^2}+\sigma_i(s)\log\frac{\sigma_i(s)+1}{\sigma_i(s)-1}\Bigg), \tag{43}$$

given here in dimensional regularization for the modified minimal subtraction scheme ($\overline{\rm MS}$) scheme, and $\sigma_i(s)=\sqrt{1-4M_i^2/s}$. In what follows, we will set the regularization scale $\mu=1.08$ GeV. Of course, observables do not depend on this choice, and we could choose another value for μ. However, the original investigation of meson-meson scattering transitions and decays by Oller and Oset [60] uses a three-momentum cutoff in the pion loop function. Translated to dimensional regularization, this gives the stated value of μ. For energies above the threshold of the state i, unitarity implies the following relation between the form factors and the isospin-zero scattering T-matrix,

$$\text{Im}\ \Gamma(s)=T(s)\cdot\frac{Q(s)}{8\pi\sqrt{s}}\cdot\Gamma^*(s), \tag{44}$$

employing an obvious matrix notation with

$$Q(s)=\begin{pmatrix}p_1(s)\,\theta(s-4M_1^2) & 0\\ 0 & p_2(s)\,\theta(s-4M_2^2)\end{pmatrix},$$
$$\Gamma(s)=\begin{pmatrix}\Gamma_1(s)\\ \Gamma_2(s)\end{pmatrix}, \tag{45}$$

where $p_i(s)=\sqrt{s/4-M_i^2}$ is the modulus of the c.m. three-momentum of the state i. Substituting Im $\Gamma(s)$ with $[\Gamma(s)$

$-\Gamma(s)^*]/(2i)$ and $T(s)$ with the expression of Eq. (42) and using the properties of the matrices $g(s)$ and $K(s)$, one can express $\Gamma(s)$ as

$$\Gamma(s)=[I+K(s)\cdot g(s)]^{-1}\cdot R(s), \tag{46}$$

where $R(s)$ is a vector of functions free of any singularity. We remark that this procedure of taking the final state interactions into account is based on the work of Ref. [61]. We also wish to stress that Eq. (46) can be applied to any K-matrix without unphysical cut contributions. As the final step, one fixes the functions in the vector $R(s)$ by requiring matching of Eq. (46) to the next-to-leading order (one loop) CHPT $\pi\pi$ and $K\bar{K}$ scalar form factors. This matching ensures that for energies where CHPT is applicable, these form factors satisfy all the requirements given by chiral symmetry and the underlying power counting. The matching procedure thus determines the vector $R(s)$, as detailed in Ref. [10]. For completeness, we give the expression for R_1^n pertinent to the scalar form factor $\Gamma_1^n(s)$,

$$R^n(s)_1=\sqrt{\frac{3}{2}}\Bigg\{1+\frac{4(L_5^r+2L_4^r)}{F_\pi^2}s+\frac{16(2L_8^r-L_5)}{F_\pi^2}M_\pi^2 +\frac{8(2L_6^r-L_4^r)}{F_\pi^2}(2M_K^2+3M_\pi^2)-\frac{M_\pi^2}{32\pi^2F_\pi^2}-\frac{1}{3}\mu_\eta\Bigg\}, \tag{47}$$

where we have used the Gell-Mann–Okubo relation $3M_\eta^2=4M_K^2-M_\pi^2$. This representation of the scalar form factors is valid from threshold up to energies of about 1.2 GeV. This range could be extended to higher energies by including multiparticle states. In fact, in the u channel with $t\sim M_\rho^2$ one encounters larger values of $\sqrt{s}$. Therefore, we simply match our representation at $\sqrt{s_0}=1.2$ GeV to the following asymptotic forms:

$$\mathrm{Re}\,\Gamma_1^n(s)\to\frac{a}{s},\qquad \mathrm{Im}\,\Gamma_1^n(s)\to\frac{b}{s^2},\qquad s\to\infty. \tag{48}$$

We have checked that the final results are insensitive to this choice of the matching point. The asymptotic form of the real part of the scalar form factor follows from quark counting rules [62] in the crossed channel; it has also been found in the dispersion analysis of the Higgs decay into two pions [56]. For continued contact with Ref. [9] we match to the asymptotic form of the vertex function of Eq. (32); a more precise treatment, if it were warranted, would involve smoothly letting $K(s)\to 0$ and solving for the form factors in a manner consistent with unitarity—for further discussion, see Ref. [56]. In Fig. 3 we display the scalar form factor $\Gamma_1^n(s)$ for $\sqrt{s}\leq 1.2$ GeV. In the low-energy region, the modulus of the form factor has its maximum at $\sqrt{s}\simeq 0.46$ GeV, very close to the central value of the σ meson mass deduced by the E791 Collaboration from analyzing the $D\to 3\pi$ data. In fact, since we wish to examine the consequences of using the more general vertex, Eq. (34), as compared to the choice Eq. (32), used by Ref. [9], we have fixed the normalization constant χ such that $\mathrm{Re}\;\Gamma_1^n(s)$ has the same value as the Breit-Wigner representation at $\sqrt{s}=0.478$ GeV. This amounts to setting $\chi=20.0$ GeV^{-1}. The peak at $\sqrt{s}\simeq 1$ GeV is due to the $f_0(980)$ and the opening of the $\bar{K}K$ channel. Also shown in Fig. 3 is the scalar form factor generated using the Breit-Wigner form with a running width, adopted in Refs. [8,9]. The differences between this form factor and that deduced from the low-energy effective field theory of QCD are marked. In particular, in Fig. 3 we see that the Breit-Wigner representation of $\Gamma_{\sigma\pi\pi}$ is deficient in that (i) $\mathrm{Im}\,\Gamma_{\sigma\pi\pi}(s)$ has a different shape as s approaches physical threshold, $s\to 4M_\pi^2$ and (ii) $\mathrm{Re}\,\Gamma_{\sigma\pi\pi}(s)$ does not possess a unitarity cusp at $s=4M_\pi^2$. It is also of the wrong sign in this limit. Moreover, the shapes of the two form factors are very different above $\sqrt{s}\simeq 0.5$ GeV—this has particular consequence for the $B\to\rho\pi$ analysis.

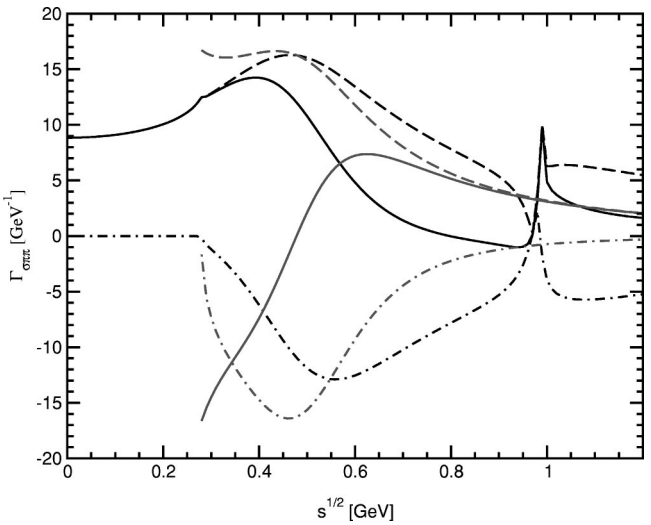

FIG. 3. The $\sigma\to\pi^+(p_+)\pi^-(p_-)$ form factor $\Gamma_{\sigma\pi\pi}$ as a function of $\sqrt{s}$, with $s=(p_++p_-)^2$. The real (solid line) and imaginary (dot-dashed line) parts of $\Gamma_{\sigma\pi\pi}$, as well as its modulus (dashed line), are shown. The curves which do not persist below the physical threshold, $\sqrt{s}=2M_\pi\sim 0.27$ GeV, correspond to the form factor adopted in Ref. [9], whereas the curves which extend to $s=0$ correspond to the form factor adopted here [10].

VI. VECTOR FORM FACTOR

Thus far we have considered the σ meson contribution to $B\to\pi^+\pi^-\pi$ decay. In this section we turn to the ρ meson contribution, $B(p_B)\to\rho\pi\to\pi^+(p_+)\pi^-(p_1)\pi(p_2)$, which presumably dominates for $t\simeq M_\rho^2$. In analogy to Eq. (29), the amplitude for $B\to\pi^+\pi^-\pi$ decay as mediated by the ρ resonance, $A_\rho(B\to\pi^+\pi^-\pi)$, is the product of a $B\to\rho\pi$ amplitude and a $\rho\to\pi\pi$ vertex function, $\Gamma_{\rho\pi\pi}$. We give the relevant formulas for $B\to\rho\pi\to\pi^+\pi^-\pi$ decay in the Appendix. In this section we focus on the construction of $\Gamma_{\rho\pi\pi}$, generating a form which is consistent with all known theoretical constraints. We detail our procedure, as the form of $\Gamma_{\rho\pi\pi}$ is important to the goals of the $B\to\rho\pi$ analysis: it drives the size of the interference between ρ states produced

in different regions of the Dalitz plot. Our vertex function differs from that of Ref. [16], as the latter adopt a Breit-Wigner form. We also compare our form with that adopted in Ref. [7]. At this point we should mention that the numerical differences are not large—simply because the pion vector form factor can be described fairly well by a Breit-Wigner form. We also note that a unitarized version of the vector form factor starting from tree-level CHPT, including resonance fields, has been presented in Ref. [63], based on the methods described in Sec. V. It could be used equally well as the parametrization employed here.

The vector form factor $F_\rho(s)$ can be directly determined from $e^+e^-\to\pi^+\pi^-$ data in the ρ resonance region. General theoretical constraints guide its construction: charge conservation requires $F_\rho(0)$ to be unity, and time-reversal invariance and unitarity lead to the identification of the phase of $F_\rho(s)$ with the $l=1$, $I=1$ $\pi\pi$ phase shift, $\delta_1^1(s)$, in the region where $\pi\pi$ scattering is elastic, $s\lesssim(M_\pi+M_\omega)^2$. Moreover, $F_\rho(s)$ is an analytic function in the complex s plane, with a branch cut along the real axis beginning at the physical threshold $s=4M_\pi^2$. Below the two-pion cut at $s=4M_\pi^2$, the vector form factor is real. Furthermore, at small s the form factor can be computed in CHPT, as detailed in Refs. [50,51]. All these constraints are captured by the Muskhelishvili-Omnès (MO) integral equation [64]. For $s\lesssim(M_\pi+M_\omega)^2$, its solution can be written [65][5]

$$F_\rho(s)=P(s)\,\Omega(s), \tag{49}$$

where $P(s)$ is a real polynomial and the Omnès function, $\Omega(s)$, contains all the phase information,

$$\Omega(s)=\exp\left(\frac{s}{\pi}\int_{4M_\pi^2}^{\infty}\frac{ds}{s'}\,\frac{\phi_1(s')}{s'-s-i\epsilon}\right),$$

$$\tan\phi_1(s)\equiv\frac{\mathrm{Im}\,F_\rho(s)}{\mathrm{Re}\,F_\rho(s)}=\tan\delta_1^1(s), \tag{50}$$

where $\delta_1^1(s)$ is the phase shift of $I=1$, $L=1$ scattering. In the Heyn-Lang parametrization [65], $\Omega(s)$ is approximated by the quotient of two analytic functions, which contain polynomial pieces and the one-pion-loop expression for the ρ self-energy function. $P(s)$ is chosen to be of third order in s in Ref. [65]. We use here a recent update of the pion form factor [21], based on the Heyn-Lang parametrization. Specifically, we use the parameter set of ''solution B'' of Ref. [21], reflecting a fit to the $e^+e^-\to\pi^+\pi^-$ data in the elastic region, subject to the constraint that the model reproduces the empirical $\pi\pi$ scattering length in the $I=1$, $L=1$ channel, $a_1^1=(0.038\pm0.002)\,M_\pi^{-3}$ [67]. In what follows, we neglect the presence of the ω resonance, or effectively $\rho^0-\omega$ mixing. The latter is an important isospin-violating effect visible in the $e^+e^-\to\pi^+\pi^-$ data in the close vicinity of $s=M_\omega^2$—the fits of Ref. [21] do include it.

[5]The solution of the MO equation with inelastic unitarity, important for $s\gtrsim(M_\pi+M_\omega)^2$, has been discussed in Ref. [66].

To realize the vertex function $\Gamma_{\rho\pi\pi}(s)$, we define

$$\Gamma_{\rho\pi\pi}(s)\equiv\frac{-F_\rho(s)}{f_{\rho\gamma}}, \tag{51}$$

where, as described in the Appendix, the electromagnetic coupling constant of the ρ meson, $f_{\rho\gamma}$, is $f_{\rho\gamma}=0.122\pm0.001\mathrm{GeV}^2$ [68]. Reference [16] adopts a Breit-Wigner form for the vertex function, namely

$$\Gamma_{\rho\pi\pi}^{\mathrm{BW}}(s)=\frac{g_\rho}{s-M_\rho^2+i\Gamma_\rho M_\rho}, \tag{52}$$

with the parameters $g_\rho=5.8$ and $\Gamma_\rho=150$ MeV—we use $M_\rho=769.3$ MeV [69]. The two forms are compared in Fig. 4—the Breit-Wigner form offers a reasonable description of the vector form factor, though differences can be seen. In particular, the imaginary part of the Breit-Wigner form does not vanish below physical threshold, as it ought. This deficiency can be repaired by giving the Breit-Wigner form a running width, i.e.,

$$\Gamma_{\rho\pi\pi}^{\mathrm{RW}}(s)=\frac{g_\rho}{s-M_\rho^2+i\Pi(s)}, \tag{53}$$

$$\Pi(s)=\frac{M_\rho^2}{\sqrt{s}}\left(\frac{p(s)}{p(M_\rho^2)}\right)^3\Gamma_\rho, \tag{54}$$

where $p(s)=\sqrt{s/4-M_\pi^2}$. This form, modulo the proportionality constant, is adopted by Ref. [7]. Figure 5 compares Eqs. (51) and (53)—the two forms are really very similar, though

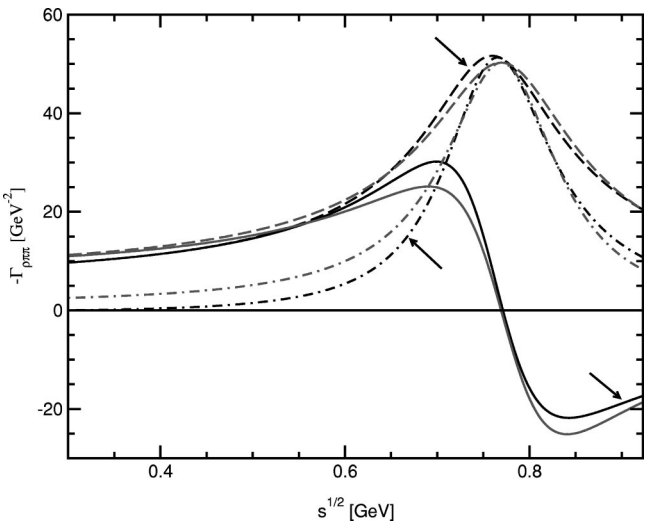

FIG. 4. The $\rho\to\pi^+(p_+)\pi^-(p_-)$ form factor $-\Gamma_{\rho\pi\pi}$ as a function of $\sqrt{s}$, with $s=(p_++p_-)^2$. The form factor is shown in the region for which $l=1$, $I=1$ $\pi\pi$ scattering is elastic. The real (solid line) and imaginary (dot-dashed line) parts of $\Gamma_{\rho\pi\pi}$, as well as its modulus (dashed line), are shown. Noting Eq. (51), the arrows indicate the form factor given by $F_\rho(s)/f_{\rho\gamma}$, as detailed in Sec. VI, whereas the other curves correspond to the Breit-Wigner form $-g_\rho/(s-M_\rho^2+iM_\rho\Gamma_\rho)$, adopted in Ref. [16].

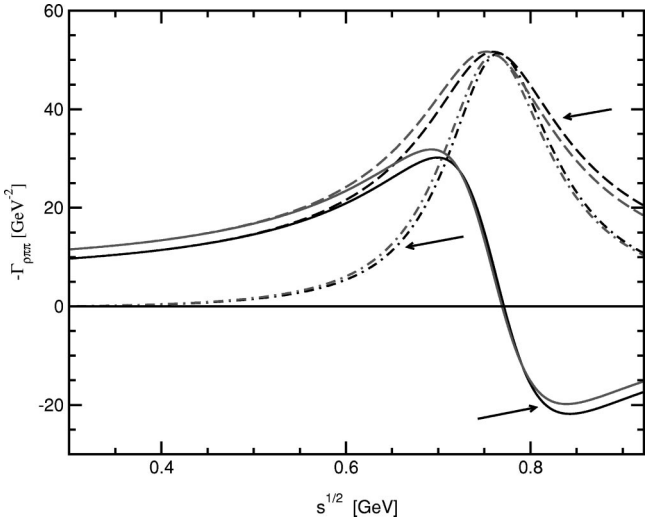

FIG. 5. The $\rho \to \pi^+(p_+)\pi^-(p_-)$ form factor $-\Gamma_{\rho\pi\pi}$ as a function of $\sqrt{s}$, with $s=(p_+ + p_-)^2$. The form factor is shown in the region for which $l=1$, $I=1$ $\pi\pi$ scattering is elastic. The real (solid line) and imaginary (dot-dashed line) parts of $\Gamma_{\rho\pi\pi}$, as well as its modulus (dashed line), are shown. Noting Eq. (51), the arrows indicate the form factor given by $F_\rho(s)/f_{\rho\gamma}$, whereas the other curves correspond to the form of Eq. (53) adopted in Ref. [7].

the forms differ slightly as $s \to 4M_\pi^2$. The phase of the form factors, namely $\tan^{-1}((\mathrm{Im}\Gamma_{\rho\pi\pi})/(\mathrm{Re}\Gamma_{\rho\pi\pi}))$, is plotted in Fig. 6. Unitarity and time-reversal invariance dictates that the phase be that of $I=1$, $L=1$ scattering; the phase shifts from the data of Refs. [70,71] are shown for comparison. The forms of Eq. (51) and Eq. (53) confront the phase shift data nicely. The agreement of the latter form is a particular surprise, as it contains only two free parameters. Apparently

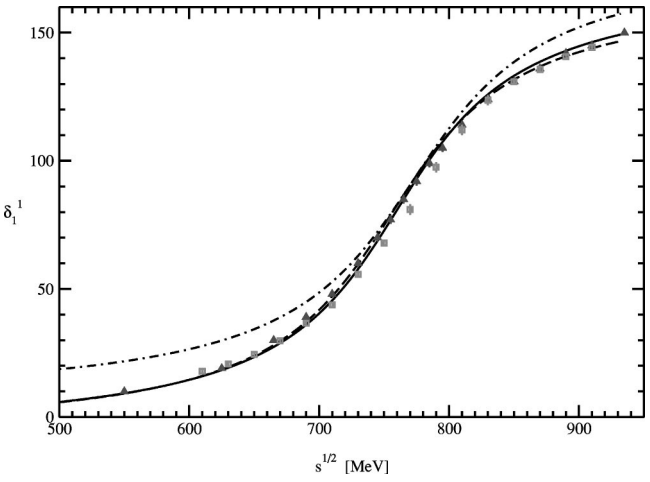

FIG. 6. The phase of the vector form factor $\Gamma_{\rho\pi\pi}(s)$ as a function of $\sqrt{s}$, in the region where the scattering is elastic. The form factor we adopt, $F_\rho(s)/f_{\rho\gamma}$ (solid line), the relativistic Breit-Wigner form of Ref. [16] (dot-dashed line), as well as that of Ref. [7] (dashed line), are all shown. Unitarity and time-reversal invariance requires that the phase be the phase shift δ_1^1 of $I=1$, $L=1$ π-π scattering. The empirical phase shifts of Ref. [70] ($\Box$) and Ref. [71] ($\triangle$) are indicated.

the form of the imaginary part is precisely captured by the $\pi\pi$ branch cut, so that the phase is accurately determined by an arctan prescription to unitarize the amplitude. This is also realized in the CHPT analysis including an explicit ρ meson, for details see Ref. [72].

In the application to follow, we need to evaluate $\Gamma_{\rho\pi\pi}(s)$ for $s>(M_\pi+M_\omega)^2$, so that at $\sqrt{s}=(M_\pi+M_\omega)\simeq 920$ MeV, the form factor of Eq. (51) is matched to the Breit-Wigner form of Eq. (52), yielding $\mathrm{Re}\,F_\rho(s)\sim a'/s$ and $\mathrm{Im}\,F_\rho(s)\sim b'/s^2$ for large s. We now turn to a discussion of our numerical results in ρ and σ-mediated $B\to 3\pi$ decay.

VII. RESULTS AND DISCUSSION

First, we must collect parameters. For crisp comparison with Refs. [9,16], we adopt the parameters used therein but reiterate them here for convenience. For meson masses and widths we use $M_B=5.279$ GeV, $M_\pi=139.57$ MeV, $M_\rho=769.3$ MeV, $\Gamma_\rho=150$ MeV, $M_\sigma=478$ MeV, and $\Gamma_\sigma=324$ MeV. We neglect the B^+, B^0 lifetime difference and use $\tau_B=1.6\times 10^{-12}$ sec. For quark masses, we use $m_b=4.6$ GeV and $\hat{m}=6$ MeV. As for the CKM matrix elements, we adopt the Wolfenstein parametrization [73], retaining terms of $\mathcal{O}(\lambda^3)$ in the real part and of $\mathcal{O}(\lambda^5)$ in the imaginary part, using $A=0.806$, $\rho=0.05$, $\eta=0.36$, and $\lambda=0.2196$. For the Wilson coefficients, we use $C_1=1.100$, $C_2=-0.226$, $C_3=0.012$, $C_4=-0.029$, $C_5=0.009$, and $C_6=-0.033$, after Ref. [44]. For form factors and coupling constants we use $F_0^{(B\to\sigma)}(M_\pi^2)=0.46$, after Ref. [74], $F_1^{(B\to\pi)}(M_\rho^2)=0.37$, $A_0^{(B\to\rho)}(M_\pi^2)=0.29$, $f_\pi=\sqrt{2}(92.4$ MeV$)\simeq 131$ MeV, and $f_\rho=0.15$ GeV^2. Finally, we use $g_\rho=5.8$ and $g_{\sigma\pi\pi}=2.52$ GeV when using the form factors of Refs. [9,16].

Let us begin by computing the branching ratios for $B\to\rho\pi$ and $B\to\sigma\pi$ decay. Assuming two-body phase space, we use Eqs. (A2) and (A3) with Eqs. (A10)–(A13), as well as Eq. (25). The results are tabulated in the first row of Table I. In the treatment of Ref. [16], the branching ratios of $B\to M_1M_2$ decay and its charge conjugate are identical, even with penguin contributions, as no strong phase between the amplitudes of differing weak phase has been included.

Proceeding to treat $B\to\rho\pi\to 3\pi$ and $B\to\sigma\pi\to\pi^+\pi^-\pi$ decay, we follow the ρ and σ intermediate states to their $\pi\pi$ final states. We realize the transition amplitudes as per Eq. (A4), (A5), or (29), and integrate over the three-body phase space as per Eq. (37), computing the integral in t over $[2M_\pi, M_B-M_\pi]$. With this procedure, the branching ratios for $B\to\rho^-\pi^+$, $B\to\rho^+\pi^-$, and $B\to\rho^0\pi^0$ become identical; we simply report the final result in the $B\to\rho^-\pi^+$ column. In treating $B^-\to\pi^+\pi^-\pi^-$ decay, we divide the total rate by 1/2, to compensate for integrating over equivalent configurations. Noting that $\mathrm{Br}(\sigma\to\pi^+\pi^-)\simeq 2/3$, the quantity in brackets in the first row includes the factor of 2/3, for comparison with the three-body results. Comparing the two-body branching ratios with those computed by integrating over the entire three-body phase space, it is evident that the branching ratios do not agree. The deviations can be attributed to both interference effects and finite-width effects.

TABLE I. Branching ratios (in units of 10^{-6}) for $B\to\rho\pi$ and $B\to\sigma\pi$ decay, computed at tree level. The numbers in parentheses include penguin contributions as well, after Ref. [16]. The first row of numbers compute the branching ratios using two-body phase space. Although $\mathrm{Br}(\rho\to\pi^+\pi^-)\simeq 1$, $\mathrm{Br}(\sigma\to\pi^+\pi^-)\simeq 2/3$, so that the numbers in brackets reflect the branching ratio times 2/3. The rows labeled "3-body" compute $B\to\rho\pi\to 3\pi$ and $B\to\sigma\pi\to\pi^+\pi^-\pi$ decay, integrating over the entire three-body phase space. "BW" denotes the use of the form factors of Refs. [9,16], Eqs. (32), (52), whereas "RW" denotes the use of the vector form factor of Ref. [7], Eq. (53). Finally, "*" denotes the use of the form factors we have advocated.

	$\overline{B}^0\to\rho^-\pi^+$	$\overline{B}^0\to\rho^+\pi^-$	$\overline{B}^0\to\rho^0\pi^0$	$B^-\to\rho^0\pi^-$	$B^-\to\sigma\pi^-$	$\overline{B}^0\to\sigma\pi^0$
2-body	21.6 (21.0)	5.96 (5.94)	0.237 (0.308)	4.74 (5.00)	15.6 [10.4]	0.147 [0.0982]
3-body (BW)	22.5 (22.1)			4.11 (4.33)	8.31	0.0739
3-body (RW)	22.4 (22.0)			4.08 (4.30)		
3-body (*)	22.3 (21.9)			4.03 (4.25)	11.7	0.108

As an example of the former, both the diagrams illustrated in Figs. 1 and 2, as well as those with $p_1\leftrightarrow p_2$, contribute to $B^-\to\pi^+\pi^-\pi^-$ decay. Clearly the interference of these diagrams is not included when the $B^-\to\rho^0\pi^-$ or $B^-\to\sigma\pi^-$ process is treated as a two-body decay. As an illustration of the latter, note that the couplings g_ρ and $g_{\sigma\pi\pi}$ are typically chosen so that they reproduce the $\rho\to\pi\pi$ and $\sigma\to\pi^+\pi^-$ decay rates, namely

$$\frac{2}{3}\Gamma_\sigma=\Gamma(\sigma\to\pi^+\pi^-)=\frac{1}{16\pi M_\sigma^2}(M_\sigma^2-4M_\pi^2)^{1/2}|g_{\sigma\pi\pi}|^2 \tag{55}$$

and

$$\Gamma_\rho=\frac{1}{48\pi M_\rho^2}(M_\rho^2-4M_\pi^2)^{1/2}|g_\rho|^2. \tag{56}$$

For the meson masses and widths we have used, these formulas yield $g_{\sigma\pi\pi}=2.53$ and $g_\rho=6.03$, respectively. Adopting these couplings in place of those used in Refs. [9,16] does reduce the discrepancy. Note that it is a "finite width" effect in that reducing the numerical width of the ρ or σ meson, in concert with Eqs. (55), (56), reduces the discrepancy between the two-and three-body treatments. It is worth noting, however, for the physical values of the meson widths, that there is no one fixed coupling $g_{\sigma\pi\pi}$ or g_ρ which removes the discrepancy entirely—the needed coupling in any given case is sensitive to the form factor chosen, as well as to the masses of the other particles in the final state. The former is apparent from a comparison with the vector form factor of Ref. [7], Eq. (53), for which we use $g_\rho=5.8$ as well. The normalization issue of which we speak is particularly relevant for the comparison of theoretical branching ratios, for $B\to VP$ decay, e.g., to experiment. It is present regardless of the form factor used. That is, in the case of the vector form factor we adopt, Eq. (51), the determination of $f_{\rho\gamma}$ can also be modified by finite width effects. The sign and size of the mismatch between the two- and three-body phase space calculations can be quite sensitive to the choice of form factor,

TABLE II. Effective branching ratios (in units of 10^{-6}) for $B\to\rho\pi$ decay, computed at tree level. The numbers in parentheses include penguin contributions as well, after Ref. [16]. The form factors are defined as in Table I.

δ [MeV] (f.f.)	$\overline{B}^0\to\rho^-\pi^+$	$\overline{B}^0\to\rho^+\pi^-$	$\overline{B}^0\to\rho^0\pi^0$	$B^-\to\rho^0\pi^-$	$\mathcal{R}$
200 (BW)	15.1 (14.7)	4.21 (4.24)	0.508 (0.497)	3.50 (3.68)	5.5 (5.1)
300 (BW)	16.4 (16.0)	4.74 (4.76)	0.918 (0.908)	3.89 (4.10)	5.4 (5.1)
200 (RW)	15.1 (14.8)	4.19 (4.21)	0.468 (0.463)	3.49 (3.68)	5.5 (5.2)
300 (RW)	16.4 (16.0)	4.69 (4.70)	0.835 (0.831)	3.87 (4.07)	5.5 (5.1)
200 (*)	15.3 (14.9)	4.26 (4.28)	0.473 (0.467)	3.49 (3.68)	5.6 (5.2)
300 (*)	16.4 (16.0)	4.75 (4.76)	0.865 (0.859)	3.85 (4.06)	5.5 (5.1)
δ [MeV] (f.f.)	$B^0\to\rho^+\pi^-$	$B^0\to\rho^-\pi^+$	$B^0\to\rho^0\pi^0$	$B^+\to\rho^0\pi^+$	$\overline{\mathcal{R}}$
200 (BW)	15.1 (14.7)	4.21 (4.15)	0.508 (0.615)	3.50 (3.68)	5.5 (5.1)
300 (BW)	16.4 (16.0)	4.74 (4.67)	0.918 (1.02)	3.89 (4.10)	5.4 (5.0)
200 (RW)	15.1 (14.7)	4.19 (4.13)	0.468 (0.571)	3.49 (3.68)	5.5 (5.2)
300 (RW)	16.4 (15.9)	4.69 (4.62)	0.835 (0.935)	3.87 (4.07)	5.5 (5.0)
200 (*)	15.3 (14.8)	4.26 (4.20)	0.473 (0.576)	3.49 (3.68)	5.6 (5.2)
300 (*)	16.4 (15.9)	4.75 (4.68)	0.865 (0.963)	3.85 (4.06)	5.5 (5.1)

TABLE III. Effective branching ratios (in units of 10^{-6}) for $B\to\sigma\pi$ and $B\to\rho\pi$ decay, computed at the tree level. The form factors are defined as in Table I.

δ [MeV] (f.f.)	$B^-\to\sigma\pi^-$	$B^-\to(\rho^0+\sigma)\pi^-$	$\overline{B}^0\to\sigma\pi^0$	$\overline{B}^0\to(\rho^0+\sigma)\pi^0$	$\mathcal{R}$
200 (BW)	2.97	6.16	0.0258	0.516	3.1
300 (BW)	5.17	8.61	0.0457	0.940	2.5
200 (RW)	2.97	6.19	0.0258	0.475	3.1
300 (RW)	5.17	8.62	0.0457	0.855	2.4
200 (*)	4.11	7.61	0.0396	0.508	2.6
300 (*)	7.01	10.7	0.0663	0.916	2.0

as illustrated by the scalar case. We set the normalization of the form factor of Sec. V, denoted by "*" in the tables, to that of the form factor of Ref. [9], Eq. (32). This is the only manner in which the parameters M_σ,Γ_σ enter our analysis. Were we to determine the normalization so that the two- and three-body computations of the $\overline{B}^0\to\sigma\pi^0\to\pi^+\pi^-\pi^0$ branching ratio yield identical results, the effective impact of the σ in the $\rho\pi$ phase space would be reduced by some 10%.

In Table II we report the $B\to\rho\pi\to3\pi$ branching ratios, computed in the manner of Ref. [16]. Our numerical results differ slightly from theirs (note that $B^0\leftrightarrow\overline{B}^0$ in their Table III). The upshot is that our estimate of $\mathcal{R}$ with penguin contributions is ~5.1, rather than the 5.5 they estimate. We show the branching ratios computed for differing vector form factors; these differing choices have little impact on the resulting branching ratios, or on $\mathcal{R}$.

We compute the $B\to\sigma\pi$ branching ratios in Table III. In this case our computed branching ratios, for $B^-\to\sigma\pi^-$ decay, are a factor of two larger with the same form factors and parameters input, as our formula, Eq. (30), differs from theirs by a factor of $\sqrt{2}$. Thus the impact of the σ in the $\rho^0\pi^-$ phase space is rather larger than that estimated in Ref. [9]. Updating the scalar form factor to use what we feel is its best estimate, we find that the values of $\mathcal{R}$ are smaller still. Interestingly, the computed values of $\mathcal{R}$ are comparable to the empirical results, albeit the errors are large. (An additional contribution to the phenomenological value of $\mathcal{R}$, realized through a diagram mediated by the a_1^- meson, is proposed in Ref. [75].)

Turning to $B\to\sigma\pi^0$ decay, we see that the contribution of the σ meson to $B^0(\overline{B}^0)\to\rho\pi$ decay is *much* smaller—with the scalar form factor we advocate, the effect is some 10%. Interestingly the σ has a tremendous impact on $B^-\to\rho^0\pi^-$ decay, and a relatively modest one on $\overline{B}^0\to\rho^0\pi^0$ decay. Let us emphasize that we have realized our numerical analysis at tree level. It is the relative size of the penguin contributions in $\overline{B}^0\to\sigma\pi^0$ and $\overline{B}^0\to\rho^0\pi^0$ decay which is of relevance to the isospin analysis to extract α. The presence of the $\sigma\pi^0$ final state in the $\rho^0\pi^0$ phase space can break the assumed relationship, Eq. (9), between the penguin contributions in $\rho\pi$ and thus mimic the effect of isospin violation—alternatively we can expand the $\rho\pi$ analysis to include the $\sigma\pi$ channel. Nevertheless, we expect our estimates to be crudely indicative of the importance of these effects—quantitatively, however, differences may exist. It is worth noting that the $\sigma\pi^0$ and $\rho^0\pi^0$ contributions can, to some measure, be distinguished. Certainly the $\sigma\pi^0$ and $\rho\pi^0$ contributions behave differently under the cut on the invariant mass of the $\pi^+\pi^-$ pair, recalling Eq. (37). Moreover, making a cut on the helicity angle θ, defined in Eq. (36), ought to also be helpful in separating the ρ^0 and σ contributions. This is illustrated in Figs. 7 and 8. The $\rho^0\pi$ contributions roughly follow a $\cos^2(\theta)$ distribution, whereas the $\sigma\pi$ contributions are quite flat, save for the bump resulting from the $\Gamma_{\sigma\pi\pi}(u)$ term in Eq. (30). Cutting on the helicity angle θ should also help disentangle the contributions from some of the B^* resonances, discussed in Ref. [16]. The contributions of B^* resonances to the $\rho\pi$ channels should be included in a more refined analysis, but they will not alter the conclusions drawn here.

VIII. SUMMARY

In this paper, we have scrutinized the role of the σ meson in $B\to\rho\pi\to3\pi$ decay, understanding its dynamical origin in the strong pion-pion final state interactions in the scalar-isoscalar channel. The presence of the $\sigma\pi^0$ contribution in

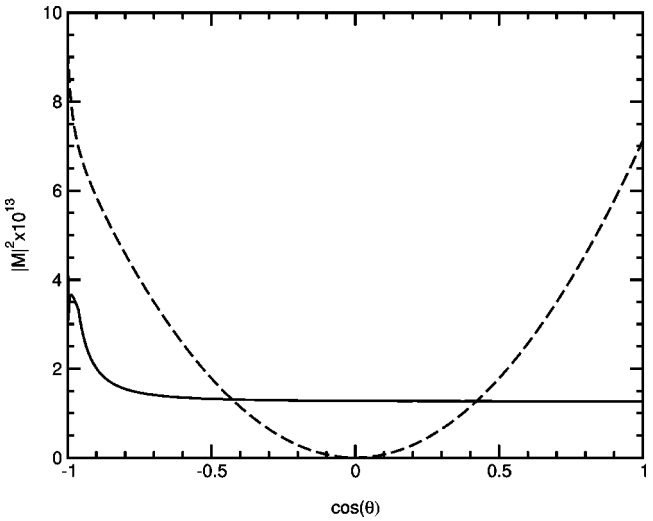

FIG. 7. Absolute square of the matrix element, $|M|^2$, for $B^-\to\rho^0\pi^-$ decay (dashed line), Eq. (A5), and for $B^-\to\sigma\pi^-$ decay (solid line), Eq. (30), as a function of $\cos\theta$ at $t=M_\rho^2$. The scalar and vector form factors advocated in Secs. V and VI have been used. The bump in the solid line reflects the presence of the $\Gamma_{\sigma\pi\pi}(u)$ term in Eq. (30).

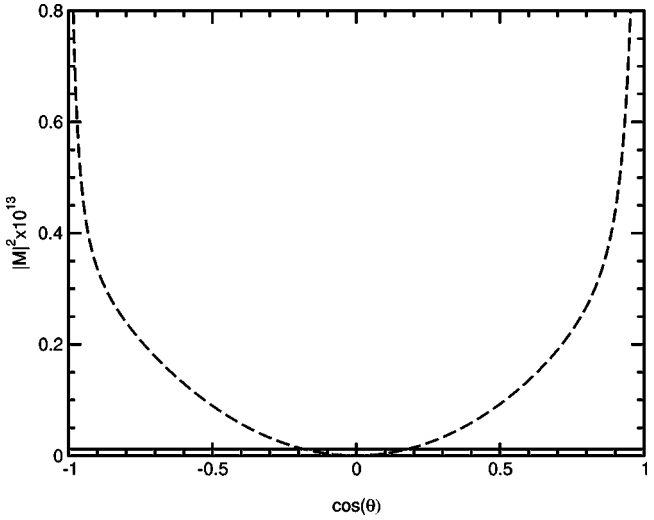

FIG. 8. Absolute square of the matrix element, $|M|^2$, for $\overline{B}^0\to\rho^0\pi^0$ decay (dashed line), Eq. (A4), and for $B^0\to\sigma\pi^0$ decay (solid line), Eq. (31), as a function of $\cos\theta$ at $t=M_\rho^2$. The scalar and vector form factors advocated in Secs. V and VI have been used.

the $\rho^0\pi^0$ phase space is important in that it can break the assumed relationship between the penguin amplitudes, Eq. (9), consequent to an assumption of isospin symmetry. In this, then, its presence mimics the effect of isospin violation. The salient results of our investigation can be summarized as follows:

(i) We have considered how SM isospin violation can impact the analysis to extract α in $B\to\rho\pi$ decay. Under the assumption that $|\Delta I|=3/2$ and $|\Delta I|=5/2$ amplitudes share the same weak phase, the presence of an additional amplitude of $|\Delta I|=5/2$ character, induced by isospin-violating effects, does not impact the $B\to\rho\pi$ analysis in any way. This is in contradistinction to the isospin analysis in $B\to\pi\pi$. Thus the isospin-violating effects of importance are those which can break the assumed relationship between the penguin contributions, Eq. (9).

(ii) The scalar form factor can be determined to good precision by combining the constraints of chiral symmetry, analyticity, and unitarity. The form factor we adopt describes the appearance of the $f_0(980)$ as well, so that the shape of the $f_0(980)$ contribution in $B\to f_0(980)\pi\to 3\pi$, e.g., should serve as a test of our approach. We emphasize that the resulting scalar form factor is very different from the commonly used Breit-Wigner form with a running width. This is in stark contrast to the vector form factor, which is dominated by the ρ resonance. In that case, one can construct simple forms that fit the theoretical and empirical constraints.

(iii) We have pointed out that the two- versus three-body treatments of the decays $B\to\rho\pi, B\to\sigma\pi$ can lead to differing results due to finite-width and interference effects.

(iv) Remarkably, the impact of the $\sigma\pi$ channel on the ratio $\mathcal{R}$, cf. Eq. (3), is huge. The numbers we find for $\mathcal{R}$ are in agreement with the empirical ones, given its sizeable experimental uncertainty. This underscores the suggestion made, as well as improves the calculations done, in Ref. [9]. Our analysis is based on *consistent* scalar and vector form factors.

(v) On the other hand, the impact of the $\sigma\pi$ channel on the $B\to\rho\pi$ isospin analysis is merely significant. Varying the cuts on the $\pi\pi$ invariant mass and helicity angle θ should be helpful in disentangling the various contributions.

(vi) We have shown that one can expand the isospin analysis to include the $\sigma\pi$ channel because it has definite properties under CP. This may be necessary if varying the cuts in the $\pi\pi$ invariant mass and helicity angle θ are not sufficiently effective in suppressing the contribution from the $\sigma\pi^0$ channel in the $\rho^0\pi^0$ phase space.

This work is merely a first step in exploiting constraints from chiral symmetry, analyticity, and unitarity in the description of hadronic B decays. In particular, the contribution of the ''doubly'' OZI-violating strange scalar form factor and its phenomenological role in factorization breaking ought be investigated.

ACKNOWLEDGMENTS

We thank H.R. Quinn for helpful discussions and M. Gronau for remarks concerning rescattering effects in B decays. We thank J.A. Oller and J. Tandean for collaborative discussions on topics germane to the issues raised here. In particular, we gratefully acknowledge J.A. Oller for the use of his scalar form factor program. S.G. thanks the SLAC Theory Group and the Aspen Center for Physics for hospitality and is supported by the U.S. Department of Energy under contract DE-FG02-96ER40989.

APPENDIX: FORMULAS FOR $B\to\rho\pi\to\pi^+\pi^-\pi^0$ DECAY

In this appendix, we report the formulas needed to evaluate $B\to\rho\pi\to\pi^+\pi^-\pi^0$ transitions, as per the approach of Sec. IV. For clarity of comparison, we conform as much as possible to the notation and conventions of Ref. [16], but give the formulas required for completeness. This also allows us to identify the changes in replacing the Breit-Wigner form adopted for the ρ resonance in Ref. [16] with the pion vector form factor we discuss in Sec. VI. Defining

$$\langle\pi^0(p_2)\pi^-(p_1)|\rho^-(p_\rho,\epsilon)\rangle=g_\rho\,\epsilon\cdot(p_2-p_1) \tag{A1}$$

and

$$\langle\rho^i(p_\rho)\pi(p_\pi)|\mathcal{H}_{\rm eff}|\overline{B}^0(p_B)\rangle=2\,\epsilon^*\cdot p_\pi\eta^i, \tag{A2}$$

$$\langle\rho^0(p_\rho)\pi^-(p_\pi)|\mathcal{H}_{\rm eff}|B^-(p_B)\rangle=2\,\epsilon^*\cdot p_\pi\tilde{\eta}^0, \tag{A3}$$

where $i\in(+,0,-)$, the $\overline{B}^0\to\rho\pi\to\pi^+\pi^-\pi^0$ amplitude can be written as

$$\begin{aligned}A_\rho(\overline{B}^0(p_B)\to\pi^+(p_+)\pi^-(p_1)\pi^0(p_2))&\\ =-\eta^0(s-u)\Gamma_{\rho\pi\pi}(t)+\eta^+(s-t)\Gamma_{\rho\pi\pi}(u)&\\ +\eta^-(t-u)\Gamma_{\rho\pi\pi}(s),&\end{aligned} \tag{A4}$$

where the first of these contributions is illustrated in Fig. 2. We have used $s=(p_1+p_2)^2$, $t=(p_+ +p_1)^2$, and $u=(p_+ +p_2)^2$, and have summed over the polarization states of the ρ^i mesons, setting $M_{\pi^\pm}=M_{\pi^0}$. With our conventions for the flavor content of the meson states, we see that $|\pi^+\rangle, |\rho^+\rangle = -|I=1\, I_3=1\rangle$, whereas the other π and ρ charge states do not have a minus sign when written in the isospin basis. Using the isospin-raising operator τ_+, we thus determine from Eq. (A1) that $\langle \pi^+(p_+)\pi^-(p_1)|\rho^0(p_\rho,\epsilon)\rangle = -g_\rho\, \epsilon\cdot(p_+-p_1)$ and $\langle \pi^+(p_+)\pi^0(p_2)|\rho^+(p_\rho,\epsilon)\rangle = g_\rho\, \epsilon\cdot(p_+-p_2)$; the signs we indicate consequently follow.[6] For the $B^-\to\rho^0\pi^-\to\pi^+\pi^-\pi^-$ amplitude we have

$$A_\rho(B^-(p_B)\to\pi^+(p_+)\pi^-(p_1)\pi^-(p_2)) = -\tilde{\eta}^0[(s-u)\Gamma_{\rho\pi\pi}(t)+(s-t)\Gamma_{\rho\pi\pi}(u)]. \tag{A5}$$

Note that $\Gamma_{\rho\pi\pi}(s)$ is the pion vector form factor, for which a Breit-Wigner form is used in Ref. [9]. As discussed in Sec. VI, we replace

$$\Gamma_{\rho\pi\pi}(x)=\frac{g_\rho}{x-M_\rho^2+i\Gamma_\rho M_\rho}\to\frac{-F_\rho(x)}{f_{\rho\gamma}}, \tag{A6}$$

where $f_{\rho\gamma}$ is the electromagnetic coupling constant of the ρ meson, determined from

$$\Gamma(\rho\to e^+e^-)=\frac{4\pi\alpha^2}{3M_\rho^3}f_{\rho\gamma}^2, \tag{A7}$$

where $\Gamma(\rho\to e^+e^-)$ is, in turn, extracted from $e^+e^-\to\pi^+\pi^-$ data at $s=M_\rho^2$, as described in Ref. [68]. For the "solution B" fit of Ref. [21] we have $f_{\rho\gamma}=0.122\pm0.001$ GeV^2 [68]. The two forms are compared in Fig. 4. In Ref. [16] the parameters $g_\rho=5.8$ and $\Gamma_\rho=150$ MeV are chosen—we use the value $M_\rho=769.3$ MeV [69] for the ρ meson mass, as it is not reported in Ref. [16].

To determine η^i, $\overline{\eta}^0$, we introduce

$$\langle\rho^-(p_\rho,\epsilon)|\overline{d}\gamma_\mu u|0\rangle=f_\rho\epsilon_\mu^*, \tag{A8}$$

$$q^\mu\langle\rho^+(p_\rho,\epsilon)|\overline{u}\gamma_\mu(1-\gamma_5)b|\overline{B}^0(p_B)\rangle = -i\,2M_\rho(\epsilon^*\cdot q)A_0^{B\to\rho}(q^2), \tag{A9}$$

where $q=p_B-p_\rho$, and recall Eqs. (23) and (24), to find

$$\eta^+=\frac{G_F}{\sqrt{2}}\left[\lambda_u a_1-\lambda_t a_4+\lambda_t\frac{a_6M_\pi^2}{\hat{m}(m_b+\hat{m})}\right]f_\pi M_\rho A_0^{B\to\rho}(M_\pi^2), \tag{A10}$$

$$\eta^-=\frac{G_F}{\sqrt{2}}[\lambda_u a_1-\lambda_t a_4]f_\rho F_1^{B\to\pi}(M_\rho^2), \tag{A11}$$

$$\eta^0=-\frac{G_F}{2\sqrt{2}}\left\{\left[\lambda_u a_2+\lambda_t a_4-\lambda_t\frac{a_6M_\pi^2}{\hat{m}(m_b+\hat{m})}\right]\times f_\pi M_\rho A_0^{B\to\rho}(M_\pi^2)+[\lambda_u a_2+\lambda_t a_4]f_\rho F_1^{B\to\pi}(M_\rho^2)\right\}, \tag{A12}$$

$$\tilde{\eta}^0=\frac{G_F}{2}\left\{\left[\lambda_u a_1-\lambda_t a_4+\lambda_t\frac{a_6M_\pi^2}{\hat{m}(m_b+\hat{m})}\right]f_\pi M_\rho A_0^{B\to\rho}(M_\pi^2) +[\lambda_u a_2+\lambda_t a_4]f_\rho F_1^{B\to\pi}(M_\rho^2)\right\}, \tag{A13}$$

where we neglect electroweak penguin contributions, as well as all isospin-violating effects. Our expressions agree with those of Ref. [9] and Ref. [15].

[6] We thank J. Tandean for discussions on this point.

[1] BABAR Collaboration, B. Aubert *et al.*, Phys. Rev. Lett. **87**, 091801 (2001).
[2] Belle Collaboration, K. Abe *et al.*, Phys. Rev. Lett. **87**, 091802 (2001).
[3] A.J. Buras, hep-ph/0109197, note Fig. 3.
[4] N. Cabibbo, Phys. Rev. Lett. **10**, 531 (1963); M. Kobayashi and T. Maskawa, Prog. Theor. Phys. **49**, 652 (1973).
[5] H.J. Lipkin, Y. Nir, H.R. Quinn, and A. Snyder, Phys. Rev. D **44**, 1454 (1991).
[6] A.E. Snyder and H.R. Quinn, Phys. Rev. D **48**, 2139 (1993).
[7] BABAR Collaboration, "The BaBar physics book: Physics at an asymmetric B factory," edited by P.F. Harrison and H.R. Quinn, SLAC-R-0504.
[8] E791 Collaboration, M. Aitala *et al.*, Phys. Rev. Lett. **86**, 770 (2001).
[9] A. Deandrea and A.D. Polosa, Phys. Rev. Lett. **86**, 216 (2001).
[10] U.-G. Meißner and J.A. Oller, Nucl. Phys. **A679**, 671 (2001).
[11] J.A. Oller, E. Oset, and A. Ramos, Prog. Part. Nucl. Phys. **45**, 157 (2000).
[12] CLEO Collaboration, C.P. Jessop *et al.*, Phys. Rev. Lett. **85**, 2881 (2000).
[13] BABAR Collaboration, B. Aubert *et al.*, hep-ex/0107058.
[14] M. Bauer, B. Stech, and M. Wirbel, Z. Phys. C **34**, 103 (1987).
[15] A. Ali, G. Kramer, and C.D. Lu, Phys. Rev. D **58**, 094009 (1998).
[16] A. Deandrea, R. Gatto, M. Ladisa, G. Nardulli, and P. Santorelli, Phys. Rev. D **62**, 036001 (2000).
[17] Y.H. Chen, H.Y. Cheng, B. Tseng, and K.C. Yang, Phys. Rev. D **60**, 094014 (1999).
[18] C.D. Lu and M.Z. Yang, hep-ph/0011238.
[19] H.R. Quinn and J.P. Silva, Phys. Rev. D **62**, 054002 (2000).
[20] T.D. Lee, *Particle Physics And Introduction To Field Theory* (Harwood, Chur, Switzerland, 1981), p. 274ff.
[21] S. Gardner and H.B. O'Connell, Phys. Rev. D **57**, 2716 (1998);

62, 019903(E) (1998), and references therein.
[22] V. Cirigliano, G. Ecker, and H. Neufeld, Phys. Lett. B **513**, 361 (2001).
[23] B. Kubis and U.-G. Meißner, Nucl. Phys. **A671**, 332 (2000); **A692**, 647(E) (2000).
[24] J.M. Flynn and L. Randall, Phys. Lett. B **224**, 221 (1989); **235**, 412(E) (1989).
[25] S. Gardner, Phys. Rev. D **59**, 077502 (1999); hep-ph/9906269.
[26] A.J. Buras and L. Silvestrini, Nucl. Phys. **B569**, 3 (2000).
[27] S. Gardner and G. Valencia, Phys. Lett. B **466**, 355 (1999).
[28] S. Gardner and G. Valencia, Phys. Rev. D **62**, 094024 (2000).
[29] CLEO Collaboration, D. Cronin-Hennessy *et al.*, hep-ex/0001010; A. Satpathy, hep-ex/0101021; BABAR Collaboration, B. Aubert *et al.*, Phys. Rev. Lett. **87**, 151802 (2001).
[30] M. Beneke, G. Buchalla, M. Neubert, and C.T. Sachrajda, Nucl. Phys. **B606**, 245 (2001).
[31] H. Leutwyler, Phys. Lett. B **378**, 313 (1996). Note that $(m_s-\hat{m})/(m_d-m_u)=40.8\pm3.2$.
[32] M. Gronau and D. London, Phys. Rev. Lett. **65**, 3381 (1990).
[33] J. Charles, Phys. Rev. D **59**, 054007 (1999).
[34] D. Pirjol, Phys. Rev. D **60**, 054020 (1999).
[35] Y. Grossman and H.R. Quinn, Phys. Rev. D **58**, 017504 (1998).
[36] M. Gronau, D. London, N. Sinha, and R. Sinha, Phys. Lett. B **514**, 315 (2001).
[37] J. Charles, A. Le Yaouanc, L. Oliver, O. Pene, and J.C. Raynal, Phys. Lett. B **425**, 375 (1998); **433**, 441(E) (1998).
[38] E687 Collaboration, P.L. Frabetti *et al.*, Phys. Lett. B **407**, 79 (1997).
[39] Y.I. Azimov, N.G. Uraltsev, and V.A. Khoze, Yad. Fiz. **45**, 1412 (1987).
[40] G. Buchalla, A.J. Buras, and M.E. Lautenbacher, Rev. Mod. Phys. **68**, 1125 (1996).
[41] M. Diehl and G. Hiller, J. High Energy Phys. **06**, 067 (2001).
[42] G. Buchalla, A.J. Buras, and M.K. Harlander, Nucl. Phys. **B337**, 313 (1990).
[43] Y.Y. Keum, H.N. Li, and A.I. Sanda, Phys. Rev. D **63**, 054008 (2001).
[44] A.J. Buras, in *Probing the Standard Model of Particle Interactions*, edited by F. David and R. Gupta (Elsevier, Amsterdam, 1999), hep-ph/9806471.
[45] G.P. Lepage and S.J. Brodsky, Phys. Lett. **87B**, 359 (1979); Phys. Rev. Lett. **43**, 545 (1979); **43**, 1625(E) (1979); G.R. Farrar and D.R. Jackson, *ibid.* **43**, 246 (1979).
[46] G.P. Lepage and S.J. Brodsky, Phys. Rev. D **22**, 2157 (1980).
[47] D.V. Bugg, I. Scott, B.S. Zou, V.V. Anisovich, A.V. Sarantsev, T.H. Burnett, and S. Sutlief, Phys. Lett. B **353**, 378 (1995).
[48] Crystal Barrel Collaboration, A. Abele *et al.*, Phys. Lett. B **380**, 453 (1996).
[49] J. Gasser and H. Leutwyler, Ann. Phys. (N.Y.) **158**, 142 (1984).
[50] J. Gasser and U.-G. Meißner, Nucl. Phys. **B357**, 90 (1991).
[51] J. Bijnens, G. Colangelo, and P. Talavera, J. High Energy Phys. **05**, 014 (1998).
[52] T.N. Truong, Phys. Rev. Lett. **61**, 2526 (1988); A. Dobado, M.J. Herrero, and T.N. Truong, Phys. Lett. B **235**, 134 (1990).
[53] J.A. Oller and E. Oset, Phys. Rev. D **60**, 074023 (1999).
[54] M. Jamin, J.A. Oller, and A. Pich, Nucl. Phys. **B587**, 331 (2000).
[55] S.N. Cherry and M.R. Pennington, hep-ph/0111158.
[56] J.F. Donoghue, J. Gasser, and H. Leutwyler, Nucl. Phys. **B343**, 341 (1990).
[57] F. Guerrero and J.A. Oller, Nucl. Phys. **B537**, 459 (1999); **B602**, 641(E) (1999).
[58] N. Kaiser, Eur. Phys. J. A **3**, 307 (1998).
[59] J. Gasser and H. Leutwyler, Nucl. Phys. **B250**, 465 (1985).
[60] J.A. Oller and E. Oset, Nucl. Phys. **A620**, 438 (1997); **A652**(E), 407 (1997).
[61] O. Babelon, J.L. Basdevant, D. Caillerie, and G. Mennessier, Nucl. Phys. **B113**, 445 (1976).
[62] S.J. Brodsky and G.R. Farrar, Phys. Rev. Lett. **31**, 1153 (1973); Phys. Rev. D **11**, 1309 (1975); V.A. Matveev, R.M. Muradyan, and A.N. Tavkhelidze, Lett. Nuovo Cimento Soc. Ital. Fis. **7**, 719 (1973).
[63] J.A. Oller, E. Oset, and J.E. Palomar, Phys. Rev. D **63**, 114009 (2001).
[64] N.I. Muskhelishvili, Tr. Tbilisi Mat. Inst. **10**, 1 (1958) [in *Singular Integral Equations*, edited by J. Radox (Noordhoff, Groningen, The Netherlands, 1953)]; R. Omnés, Nuovo Cimento **8**, 316 (1958).
[65] M.F. Heyn and C.B. Lang, Z. Phys. C **7**, 169 (1981) and references therein.
[66] T.N. Pham and T.N. Truong, Phys. Rev. D **14**, 185 (1976); Phys. Rev. D **16**, 896 (1977).
[67] M.M. Nagels *et al.*, Nucl. Phys. **B147**, 189 (1979); O. Dumbrajs *et al.*, *ibid.* **B216**, 277 (1983).
[68] S. Gardner and H.B. O'Connell, Phys. Rev. D **59**, 076002 (1999).
[69] Particle Data Group, D.E. Groom *et al.*, Eur. Phys. J. C **15**, 1 (2000).
[70] B. Hyams *et al.*, Nucl. Phys. **B64**, 134 (1973) [in π-π *Scattering-1973*, edited by P. K. Williams and V. Hagopian, AIP Conf. Proc. No. 13 (AIP, New York, 1973), p. 206]; W. Ochs, Ph.D. thesis, University of Munich, 1974.
[71] S.D. Protopopescu *et al.*, Phys. Rev. D **7**, 1279 (1973).
[72] V. Bernard, N. Kaiser, and U.-G. Meißner, Nucl. Phys. **B364**, 283 (1991).
[73] L. Wolfenstein, Phys. Rev. Lett. **51**, 1945 (1983).
[74] R. Gatto, G. Nardulli, A.D. Polosa, and N.A. Tornqvist, Phys. Lett. B **494**, 168 (2000).
[75] N. Paver and Riazuddin, hep-ph/0107330.